ChemPubSoc Europe
DOI: 10.1002/open.201500053
Open Access ChemistryOPEN Reviews

# Gated Silica Mesoporous Materials in Sensing Applications

Félix Sancenón,*[a, b, c] Lluís Pascual,[a, b, c] Mar Oroval,[a, b, c] Elena Aznar,[a, c] and Ramón Martínez-Máñez*[a, b, c]

Silica mesoporous supports (SMSs) have a large specific surface area and volume and are particularly exciting vehicles for delivery applications. Such container-like structures can be loaded with numerous different chemical substances, such as drugs and reporters. Gated systems also contain addressable functions at openings of voids, and cargo delivery can be controlled on-command using chemical, biochemical or physical stimuli. Many of these gated SMSs have been applied for drug delivery. However, fewer examples of their use in sensing protocols have been reported. The approach of applying SMSs in sensing uses another concept—that of loading pores with a reporter and designing a capping mechanism that is selectively opened in the presence of a target analyte, which results in the delivery of the reporter. According to this concept, we provide herein a complete compilation of published examples of probes based on the use of capped SMSs for sensing. Examples for the detection of anions, cations, small molecules and biomolecules are provided. The diverse range of gated silica mesoporous materials presented here highlights their usefulness in recognition protocols.

## 1 Introduction

Recent advances made in nanotechnology and in molecular and biomolecular chemistry have resulted in the design of supramolecular and biologically inspired systems capable of showing inventive related functions that fuel areas such as bioengineering, biosensing, and bionanotechnology into new horizons.[1] In this context, some new systems are based on the use of hybrid materials, obtained by anchoring organic molecules or supermolecules to certain inorganic scaffoldings.[2] In this field, one appealing application is the development of gated nanodevices for controlled delivery. In fact the development of stimuli-responsive nanoscopic hybrid gated materials, able to release an entrapped cargo when external stimuli are applied, has attracted much attention.[3] These gated materials usually contain a switchable "gate-like" ensemble capable of being "opened" or "closed" when certain external stimuli are applied, as well as a suitable inorganic support that acts as a nanocontainer (for loading the carrier). For the support, different-sized mesoporous silicas have been selected and used as inorganic scaffolds in gated ensembles thanks to their suitable properties.[4] In particular, silica mesoporous supports (SMSs) can be obtained in different sizes, from micrometric to nanometric, with tailor-made homogeneous pores of around 2-10 nm. They also show high inertness, are easy to functionalize using well-known chemistries, and have a very large specific surface area and specific volume, and therefore have remarkable load capacity.[5] While dealing with the "gate-like" ensemble, SMSs have been functionalized with a large collection of switchable molecular, supramolecular and biomolecular pore-capping ensembles to develop gated particles capable of showing a "zero release" of cargo and of delivering it upon the application of specific chemical, physical or biochemical stimuli.[6]

As stated above, these capped materials have been used mainly in drug delivery applications. In contrast, very few examples of their use in sensing protocols are available. The core concept for applying SMSs into sensing protocols is to load the support with a reporter and to design the capping mechanism in such a way that a target analyte is able to selectively trigger uncapping and the delivery of the cargo (a reporter).[7] This new sensing paradigm conceptually differs from classic supramolecular "binding site–signaling subunit" systems because the new protocol disconnects the recognition step from the signaling event, which therefore makes signaling independent of the host–guest interaction.[8] Another advantage of this protocol is the presence of amplification features. For instance, it has been reported that the presence of relatively few molecules of a certain analyte may induce the release of a relatively large quantity of entrapped dye molecules.[9] This sensing approach using gated systems offers great potential for the preparation of new sensing systems with enhanced features compared with classical signaling probes. In particular, it is possible to select, with minimum effort, different porous supports, a large range of gate-like systems, and a number of

[a] Dr. F. Sancenón, L. Pascual, M. Oroval, Dr. E. Aznar, Prof. R. Martínez-Máñez
Centro de Reconocimiento Molecular y Desarrollo Tecnológico (IDM)
Unidad Mixta Universidad Politécnica de Valencia–Universidad de Valencia (Spain)
[b] Dr. F. Sancenón, L. Pascual, M. Oroval, Prof. R. Martínez-Máñez
Departamento de Química, Universidad Politécnica de Valencia
Camino de Vera s/n, 46022 Valencia (Spain)
E-mail: rmaez@qim.upv.es
[c] Dr. F. Sancenón, L. Pascual, M. Oroval, Dr. E. Aznar, Prof. R. Martínez-Máñez
CIBER de Bioingeniería, Biomateriales y Nanomedicina (CIBER–BBN) (Spain)

reporters which display chromogenic, fluorogenic, or electrochemical responses.

When using gated concepts for sensing, two possible situations are envisioned (see Figure 1). In one, pores are open and the reporter is delivered to the solution, whereas in the presence of a given analyte, this molecule can bind to receptors on the external surface of the SMS and close the gate. As capping of the mesoporous support is selectively achieved in the presence of a target analyte, the design of a probe can be envisioned. In the second approach, the starting material is capped, and the presence of a target guest induces pore opening and dye delivery due to competitive binding. Of both these approaches, the second is perhaps the most interesting because it is able to show a signal when the reporter is released (i.e. off–on behavior), which is generally easier to measure than dye delivery inhibition (i.e. on–off behavior). However, examples of the first approach were reported first, whereas examples of the second have been reported more recently.[7]

Ramón Martínez-Máñez was born in Valencia, Spain. He received his Ph.D. in Chemistry from the University of Valencia in 1986 and was a postdoctoral fellow at Cambridge University, UK. He is a full professor in the Department of Chemistry at the Polytechnic University of Valencia. Presently, he is the director of the IDM Research Institute at the Polytechnic University of Valencia. He is the co-author of more than 300 research publications and nine patents. He is a member of the American Chemical Society. His current research interests involve developing new sensing methods for different chemicals of interest, including anions, cations and neutral species, such as explosives and chemical warfare agents. He is also involved in designing gated hybrid materials for on-command delivery applications.

Félix Sáncenón was born in 1968 in Manises, Valencia, Spain, and graduated with a degree in chemistry in 1991. He received his Ph.D. in 2003 from the Polytechnic University of Valencia, where he research the development of chromogenic and fluorogenic chemosensors for cations and anions in the group of Professor Ramón Martínez-Máñez. Afterwards, he obtained a Marie-Curie contract from the E.U. and worked with Professor Luigi Fabbrizzi at the Universitá di Pavia (Italy) on the synthesis of chromogenic receptors for ion pairs. Then, he joined the Department of Chemistry at the Polytechnic University of Valencia with a Ramón y Cajal contract. He became a lecturer in 2006. He is the co-author of more than 170 research publications. His current research interests comprise the use of hybrid materials for the development of sensors and for the construction of molecular gates.

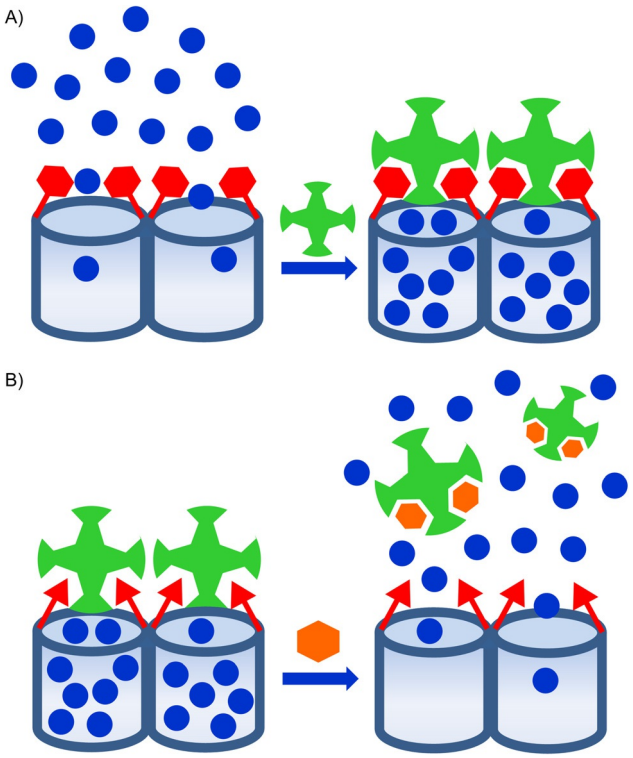


**Figure 1.** Scheme of the recognition paradigm using nanoscopic gate-like scaffoldings: A) inhibition of dye release due to analyte coordination with grafted binding sites; B) uncapping of the pores by an analyte-induced displacement reaction.

This review aims to act as a complete compilation of published examples of the design of probes based on capped silica mesoporous supports. Examples of stochastic sensors (based on nanometer-sized pores in insulating membranes),[10] simple probes based on dyes on silica mesoporous supports (using uncapped systems),[11] or electrochemical sensors constructed with mesoporous membranes[12] are not reported herein. The examples detailed below showed capped SMSs with applications in recognition protocols divided into four main sections: sensing of anions, sensing of cations, sensing of small neutral molecules, and sensing of biomolecules. Our aim was to also include capped SMSs that could be opened in the presence of certain molecules and which, in our opinion, may find use in sensing, even though they were designed for a different application in the original work.

## 2 Sensing of Anions

As far as we know, the first time it was suggested that gated SMSs could be used for sensing applications was reported by our group in 2006, and it was based on the on–off behavior shown in Figure 1 A. The system consisted of an SMS loaded with $Ru(bipy)_3^{2+}$ dye as the reporter and functionalized on the external surface with 3-[2-(2-aminoethylamino)ethylamino]-propyl trimethoxysilane. At a neutral pH, in which the experiments were carried out, the gate was open, and delivery of the ruthenium complex was detected chromo-fluorogenically.

However, presence of adenosine triphosphate (ATP), and of adenosine diphosphate (ADP) to a lesser extent, allowed the selective inhibition of indicator delivery by the formation of strong complexes between tethered polyamines and ATP anions through hydrogen bonding and electrostatic interactions (Figure 2). The system presented good selectivity for ATP in the presence of other anions, such as chloride, sulfate, or

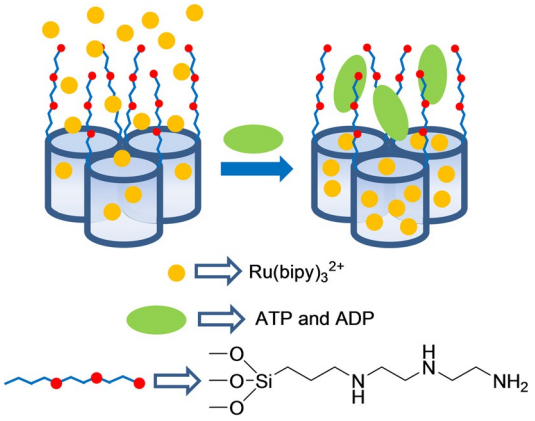


**Figure 2.** Micrometric silica mesoporous support functionalized with polyamines for the detection of ATP.

guanosine monophosphate (GMP), which were either too small or formed complexes that were too weak to effectively cap pores.[13] In a complementary study, the same authors studied the behavior of a similar amine-functionalized material obtained by anchoring suitable polyamines to pore outlets of the SMS loaded with $Ru(bipy)_3^{2+}$.[14] A pH-driven open/close mechanism was observed that emerged from a hydrogen-bonding interaction between amines at a neutral pH (open gate) and Coulombic repulsions at an acidic pH between closely located polyammoniums at pore openings (closed gate). In addition to the pH-driven protocol, the opening/closing of the gate-like ensemble could also be modulated by an anion-controlled mechanism. Choice of a certain anionic guest resulted in a different gate-like ensemble behavior, which ranged from basically no action (chloride) to complete (ATP) or partial pore blockage, depending on pH (sulfate and phosphate). The authors explained the remarkable anion-controllable response of the gate-like ensemble in terms of anion complex formation with tethered polyamines.

In another work, which also used an on–off behavior, as shown in Figure 1 A, the authors developed a hybrid SMS capable of chromo-fluorogenically detecting long-chain carboxylates by using mesoporous silica microparticles loaded with $Ru(bipy)_3^{2+}$ and functionalized on the external surface with imidazolium binding sites.[15] The release profile of the entrapped dye from the described material was tested in aqueous media at a neutral pH in the presence of different linear carboxylates ($CH_3(CH_2)_nCO_2^-$, $n=0$, 2, 4, 6, 8, and 10). It was found that short carboxylates, such as acetate, butanoate, hexanoate, and octanoate, were unable to induce pore blockage, whereas presence of larger carboxylates, such as decanoate and dodecanoate inhibited dye release, most likely due to the electrostatic interaction of these carboxylates with the imidazolium binding sites on the surface and the formation of a dense hydrophobic monolayer around pore outlets (see Figure 3). In particular, dodecanoate completely inhibited dye

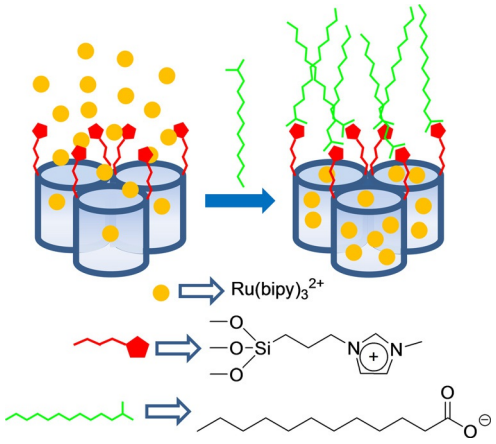


**Figure 3.** Micrometric silica mesoporous support functionalized with imidazolium binding sites for the detection of long-chain carboxylates.

delivery at the millimolar level. In a similar study, the same authors[16] developed new sensing materials, also for the optical detection of long-chain carboxylates, based on the use of SMSs loaded with $Ru(bipy)_3^{2+}$ and functionalized on the external surface with thiourea or urea binding sites. The release profile of the entrapped dye from these materials was also tested in aqueous media in the presence of different linear carboxylates ($CH_3(CH_2)_nCO_2^-$, $n=0$, 2, 4, 6, 8, and 10). In general, a similar result to that found for the solid functionalized with imidazolium was observed.

A final example, based on the open–closed protocol shown in Figure 1 A for anion sensing, was developed for the detection of borate. Using the well-known reaction between polyalcohols and borate anion to form boronate esters, the authors developed a mesoporous Mobil Composition of Matter 41 (MCM-41) support loaded with $Ru(bipy)_3^{2+}$ dye and functionalized with a saccharide derivative on the external surface.[17] Presence of borate (pH 7.0) induced pore closure, which inhibited dye delivery due to the formation of boroesters through the reaction of borate with the hydroxyl moieties of the anchored saccharides (Figure 4). The control of mass transport by borate anion was very selective; for instance, other anions (e.g. $CO_3^{2-}$, $SO_4^{2-}$, $Cl^-$, $Br^-$, $NO_3^-$, $PO_4^{3-}$) or cations (e.g. aluminum, copper, iron, sodium, potassium, and calcium ions) showed no effect. Based on this simple protocol, a limit of detection (LOD) for borate of about 70 ppb in water (HEPES, pH 7.0) was achieved.

A common characteristic of the above examples is the use of uncapped materials, which were selectively capped in the presence of certain anions by coordination of the anion with relatively small binding sites attached to the external surface of SMSs, which generally resulted in an on–off sensing protocol. In contrast to this approach, in an off–on sensing systems it is normally necessary to use large molecules to allow to pre-

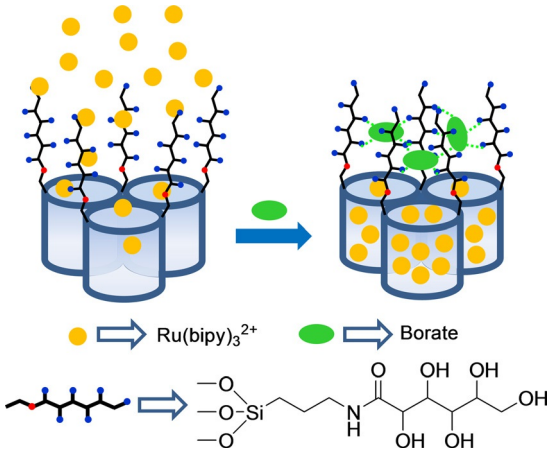


**Figure 4.** Micrometric silica mesoporous support functionalized with polyalcohols for the detection of borate.

pare capped materials, which could be opened in the presence of target analytes. One method to achieve this goal used aptamers. An example of detection of anions using this protocol was reported in 2011, by Özalp and co-workers, who paid attention to the use of aptamers to develop an ATP-responsive gated material (see Figure 5).[18] In their work, they used an

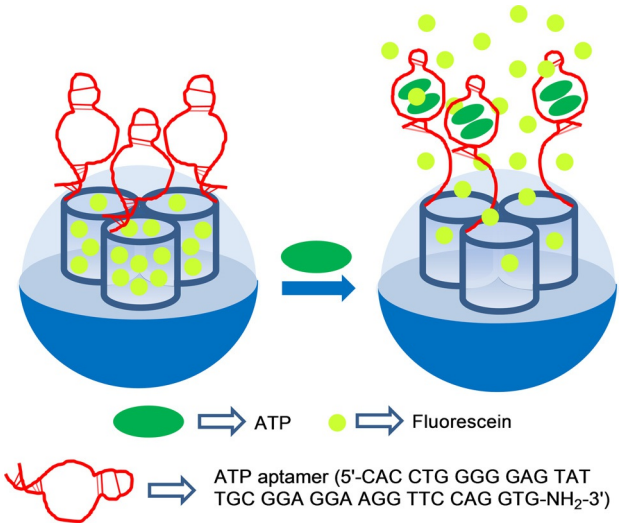


**Figure 5.** Nanometric silica mesoporous support loaded with fluorescein and capped with ATP aptamers for the detection of ATP.

amino-terminated oligonucleotide sequence (5′-CAC CTG GGG GAG TAT TGC GGA GGA AGG TTC CAG GTG-$NH_2$-3′), which contained the well-known ATP aptamer (5′-CAC CTG GGG GAG TAT TGC GGA GGA AGG TT-3′), and a short extra fragment (5′-CCA GGT G-$NH_2$-3′) to induce a hairpin-like structure that blocked pores. An SMS in the form of nanoparticles, loaded with fluorescein and functionalized on the external surface with sulfhydryl groups, was prepared and the amino functionalized aptamer was covalently attached using sulfo-*N*-succinimidyl 4-maleimidobutyrate as a crosslinker. These authors observed that the hairpin aptamer blocked pores, while presence of ATP triggered the delivery of the entrapped fluorescein dye. This was explained by ATP binding, which induced a conformational change from a duplex to a single-stranded DNA near the aptamer region, which was close to the SMS surface and resulted in fluorescein release. These authors also found that nanoparticles capped with a mutated hairpin did not respond to ATP, and that guanosine 5′-triphosphate (GTP) was also unable to trigger fluorescein release. They also confirmed that cargo delivery was dependent on ATP concentration. Later the same authors extended their previous work by focusing on monitoring the performance of aptamer-gated SMSs using circular dichroism.[19] In this new study, the same ATP aptamer as that described above was employed, but in this case a different hairpin-forming extension was used, which resulted in the final capping sequence 5′-CAC CTG GGG GAG TAT TGC GGA GGA AGG TTT TTT TCC AGG TG-$(CH_2)_6$-$NH_2$-3′.

Wang and co-workers also developed ATP-selective delivery systems using silica mesoporous nanoparticles capped with the same ATP aptamer,[20] but based on a different configuration of the gated ensemble to that used by Özalp et al. In particular, these authors functionalized SMSs with 3-cloropropyltrimethoxysilane and then transformed the chloride atom of the attached organic groups into an azide moiety by a reaction with sodium azide. On the other hand, the ATP aptamer was hybridized with two different single-stranded DNA (ssDNA) sequences (e.g. 5′-alkyne-TTC CTC CGC A-3′ and 5′-alkyne-ATA CTC CC-3′) yielding a sandwich-type DNA structure. The pores of the inorganic scaffold, functionalized with azide moieties, were loaded with $Ru(bipy)_3^{2+}$, and then the system was capped with the sandwich-type DNA structure containing the ATP aptamer sequence through a click chemistry reaction between the azide group in the solid and alkyne groups in the DNA ensemble. This allowed pores to be blocked, which inhibited dye release (Figure 6). However, upon addition of ATP, dye release was observed. Cargo delivery was studied in Tris-HCl buffer at different ATP concentrations, from 0 to 20 mM, and was monitored by fluorescence spectroscopy. The ATP-induced response was attributed to the competitive displacement of the ATP aptamer from the sandwich-type DNA via the formation of the corresponding ATP-aptamer complex. The $Ru(bipy)_3^{2+}$ reporter release was observed only when ATP was present, whereas cytosine 5′-triphosphate (CTP), GTP, and uridine 5′-triphosphate (UTP) at 20 mM were unable to induce dye delivery.

Yang and co-workers developed ATP-responsive gated materials using aptamer-containing gold nanoparticles (AuNPs) as caps (Figure 7).[21] In their work, these authors functionalized the external surface of an SMS with amino groups and, in further steps they anchored adenosine-5′-carboxylic acid moieties (via an amidation reaction) and loaded the porous network of the support with fluorescein isothiocyanate (FITC). On the other hand, AuNPs derivatized with ATP aptamer 5′-CCT GGG GGA GTA TTG CGG AGG AAG GTT-SH-3′ by forming an Au–S bond were prepared. The final sensory material was obtained by capping the loaded support pores with aptamer-functionalized AuNPs. Phosphate-buffered saline (PBS, pH 7.4) suspensions of the capped solid showed negligible dye leaching,

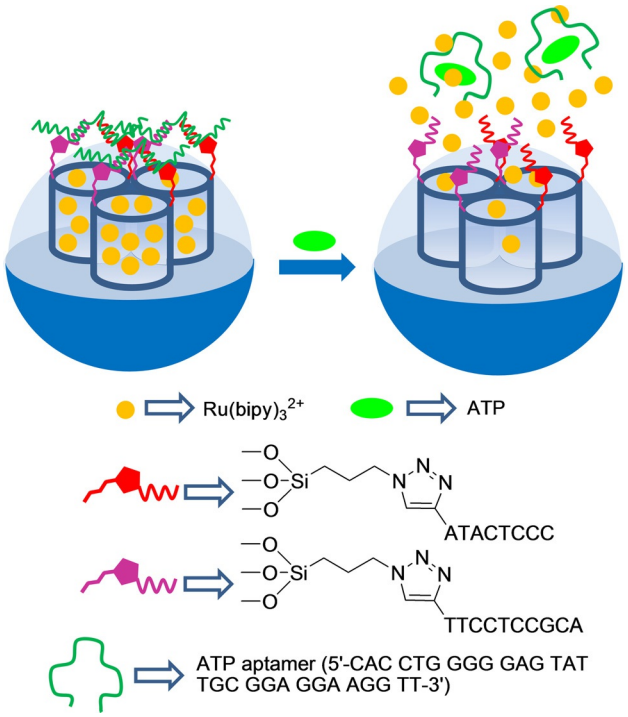


**Figure 6.** Nanometric silica mesoporous support loaded with $Ru(bipy)_3^{2+}$ and capped with ATP aptamers for the detection of ATP.

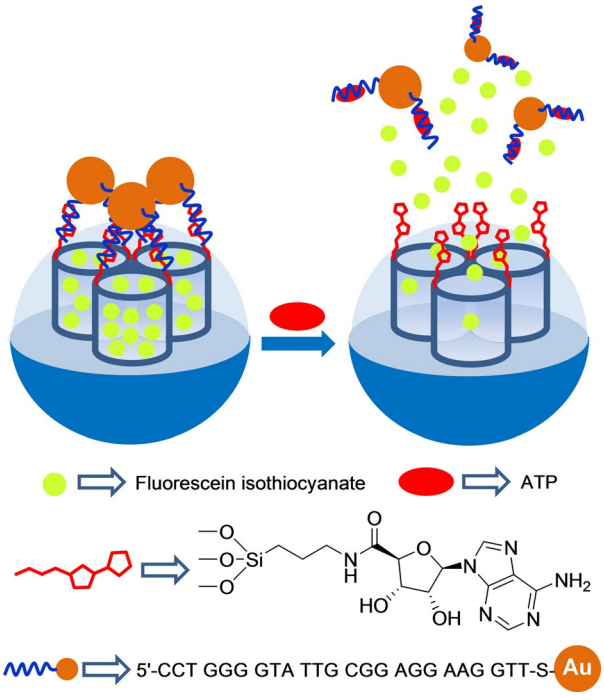


**Figure 7.** Nanometric silica mesoporous support loaded with fluorescein isothiocyanate and capped with ATP aptamer containing gold nanoparticles (AuNPs) for the detection of ATP.

whereas presence of ATP triggered the release of the FITC reporter. The authors also found that the amount of released FITC was dependent on ATP concentration (with a maximum dye release at the 8 mM ATP concentration). The uncapping process was ascribed to a competitive displacement reaction of AuNPs from the solid surface upon the coordination of ATP with the grafted aptamer. Finally, selectivity of the system using ATP analogs, such as CTP, GTP, and UTP, was studied. None of the tested analogs induced FITC reporter release. These authors also examined the uncapping ability of an oligonucleotide complementary to the ATP aptamer and a random sequence. In this case, they found remarkable dye release with the complementary sequence, which was even better than with ATP given its higher binding constant ($K_{d\ oligonucleotide}$: ~1 nM; $K_{d\ ATP}$: 0.7–0.8 μM), whereas presence of the random sequence induced negligible dye delivery.

Tang and co-workers recently developed an SMS capped with AuNPs to detect ATP by using a conventional glucometer readout and the same selective ATP aptamer as that used above by Özalp, Wang, and Yang (see Figure 8).[22] For this purpose, the authors functionalized the external surface of silica mesoporous nanoparticles with aminopropyl moieties and then linked a single-stranded sequence (e.g. 5′-$NH_2$-TTT TTA CCT TCC TCC GCA A-3′, DNA1) to amino groups using glutaraldehyde as linker. The inorganic scaffold pores were loaded

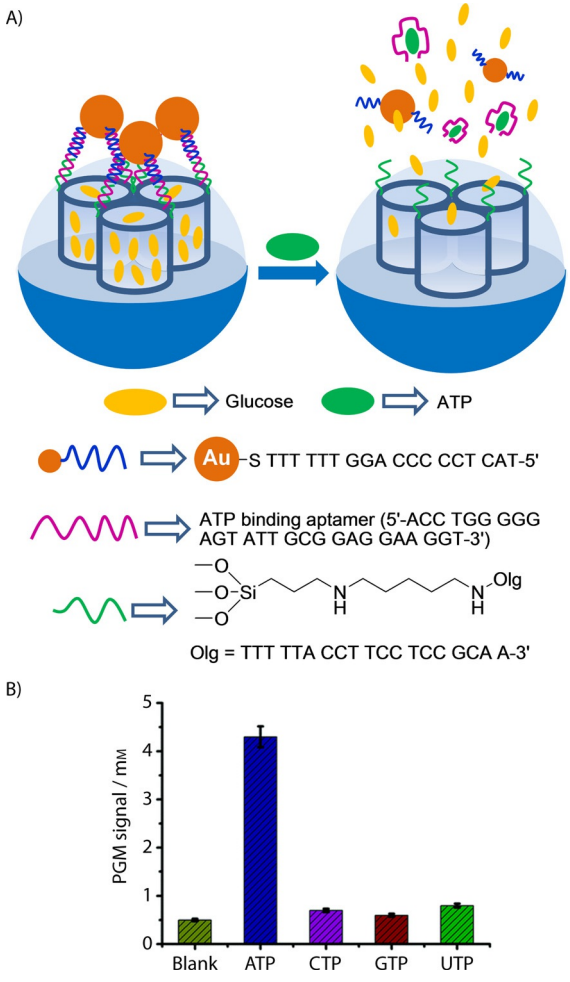


**Figure 8.** A) Nanometric silica mesoporous support loaded with glucose and capped with ATP aptamer containing AuNPs for the detection of ATP. B) Selectivity release profile for the sensing material triggered by ATP, CTP, GTP and UDP (0.1 mM after 6 h). PGM = personal glucometer. (Reproduced with permission from Ref. [22]. Copyright 2014, Royal Society of Chemistry).

with glucose. On the other hand, AuNPs were coated with another single-stranded sequence (5′-TAC TCC CCC AGG TTT TTT-SH-3′, DNA2). Both DNA1 (grafted on the outer surface of the mesoporous support and DNA2 (used as a coating of AuNPs) are complementary to the adjacent areas of the ATP aptamer sequence. In the presence of the ATP aptamer, immobilized DNA1 and DNA2 hybridized (and formed a three-stranded complex), with the subsequent pore capping by bulky AuNPs. Buffered suspensions of the capped system at pH 7.3 showed no entrapped glucose release. However in the presence of ATP, glucose release was clearly detected and was measured by a commercially available glucometer. The observed response was due to ATP binding with the aptamer, which resulted in a separation of AuNPs from the SMS and cargo delivery. The capped material was able to detect ATP within a linear range from 0.01 to 0.8 mM with an LOD of 8 μM. Presence of other nucleotides, such as CTP, GTP, and UTP, was unable to uncap pores. A similar strategy was adopted to detect cocaine (linear range from 0 to 1 mM).

## 3 Sensing of Cations

Capped mesoporous silica nanoparticles designed for the detection of small cations are scarce. As far as we know, the first example reported was designed to sense the presence of cation $CH_3Hg^+$.[23] This was, as far as we can tell, also the first example to have used an off–on approach based on the general paradigm shown in Figure 1B. The gated material consisted of a mesoporous support loaded with dye safranin O and capped with 2,4-bis-(4-dialkylaminophenyl)-3-hydroxy-4-alkylsulfanylcyclobut-2-one (APC) groups. APC moieties were readily formed by the reaction of a squaraine dye and thiol units, which were previously anchored to the external surface of the mesoporous support. When $CH_3Hg^+$ was added to the acetonitrile:toluene 4:1 *v/v* suspension of the APC-capped support, safranin O release was observed. This uncapping process derived from the reaction of methylmercury with the thiol group on APC moieties, which resulted in the coordination of the cation to thiols and, in both, the release of the bulky squaraine chromophore and the delivery of the entrapped safranin O reporter (see Figure 9). The chromogenic indication reaction allowed the detection of $CH_3Hg^+$ down to 0.5 ppm, whereas the use of standard fluorometric methods reduced the LOD to below 2 ppb. Experiments were done in acetonitrile:toluene 4:1 *v/v* mixtures to achieve discrimination from $Hg^{2+}$ given its low solubility in this medium. This procedure was successfully tested to optically determine methylmercury in fish samples by a simple extraction procedure with toluene and $CH_3Hg^+$ detection with the APC-capped solid. These real fish samples were also spiked with cations $Na^+$, $K^+$, $Ca^{2+}$, $Mg^{2+}$, $Cu^{2+}$, $Ni^{2+}$, $Zn^{2+}$, $Ag^+$, $Pd^{2+}$, $Cd^{2+}$, $Au^{3+}$, and $Tl^+$ and various organic species, for example, sodium lauryl sulfate, cysteine, histamine, ethanol, heptylamine, and hexanethiol. However, none of these species affected the response of the capped material to $CH_3Hg^+$.

More recently, Tan, Zhang, and co-workers proposed a mercury probe based on a DNA-capped SMS. MCM-41-type mesoporous silica nanoparticles were loaded with rhodamine 6G

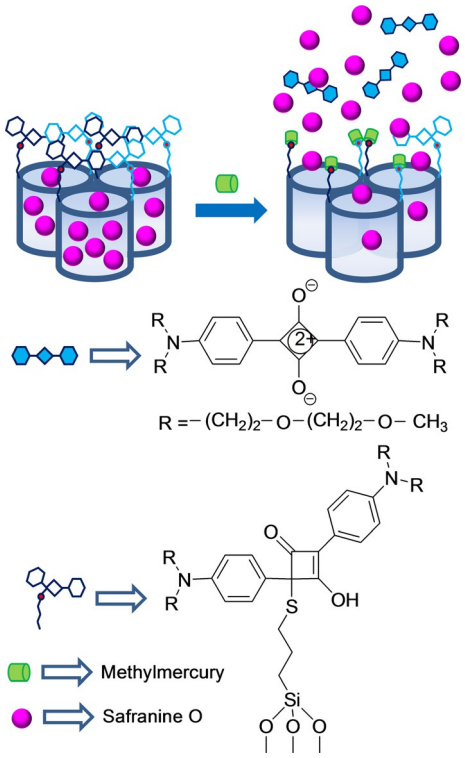


**Figure 9.** Micrometric silica mesoporous support loaded with safranine and capped with 2,4-bis-(4-dialkylaminophenyl)-3-hydroxy-4-alkylsulfanylcyclobut-2-one (APC) groups for the detection of methylmercury.

and functionalized with isocyanate moieties. Amino-modified oligonucleotide 5′-GAA GAA CAA CAA AAA-$NH_2$-3′ was then reacted with the isocyanate groups. A second larger strand (5′-GTT GTT CTT CCT TTG TTT CCC CTT TCT TTG GTT GTT CTTC-3′), complementary to the anchored one was hybridized, capping the pores of the material. This second oligonucleotide strand was very rich in thymine groups and showed a high affinity to $Hg^{2+}$. In presence of this ion, the authors found that the strand was displaced from the surface to form the corresponding $Hg^{2+}$–aptamer complex, which resulted in dye delivery (Figure 10). Quantification studies, which measured the delivered rhodamine dye fluorescence, showed that the system was able to detect $Hg^{2+}$ in water with a LOD of 4 ppb. The system was selective and no important cargo delivery was observed in the presence of other cations, for example, $Ni^{2+}$, $Pd^{2+}$, $Fe^{2+}$, $Fe^{3+}$, $Ba^{2+}$, $Zn^{2+}$, $Ca^{2+}$, $Mg^{2+}$, $Cu^{2+}$, $Co^{2+}$, and $Cd^{2+}$.[24]

In an independent work Wen, Song, and co-workers developed SMSs capped with a $K^+$-selective aptamer and demonstrated that cargo delivery can be achieved when this cation is present.[25] However, these authors did not specifically carry out sensing studies, but used the system to demonstrate the potential use of this aptamer for the design of logic gate systems.

Choi et al. reported the design of capped silica mesoporous nanoparticles capable of being opened in the presence of $K^+$ using macrocycles.[26] These authors used a SMS in the form of nanoparticles, which was loaded with curcumin dye and anchored a 18-crown-6 derivative to the external surface. Nanopar-

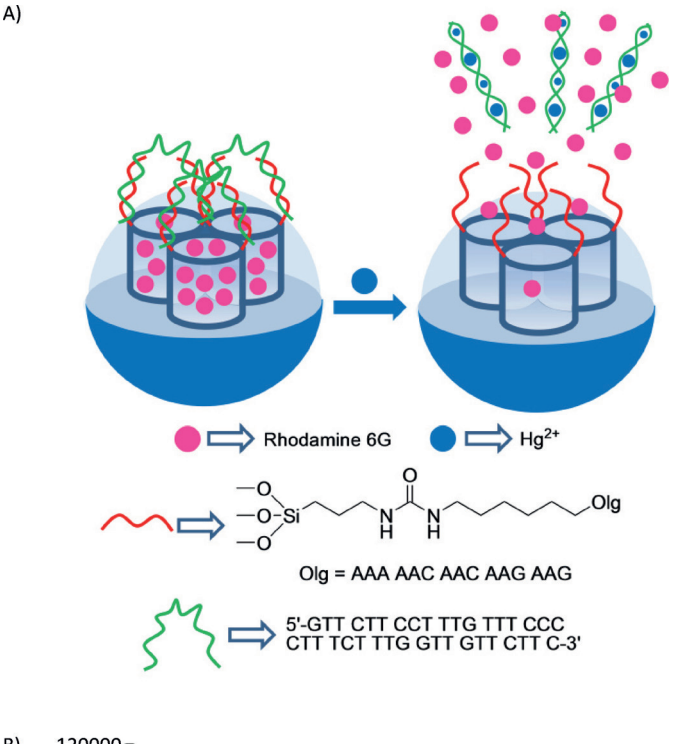


**Figure 10.** A) Nanometric silica mesoporous support loaded with rhodamine and capped with aptamers for the detection of $Hg^{2+}$ cations. B) Emission intensity in the presence of increasing quantities of $Hg^{2+}$ (Inset: linear fit of the fluorescence signal). (Reproduced with permission from Ref. [24]. Copyright 2012, American Chemical Society).

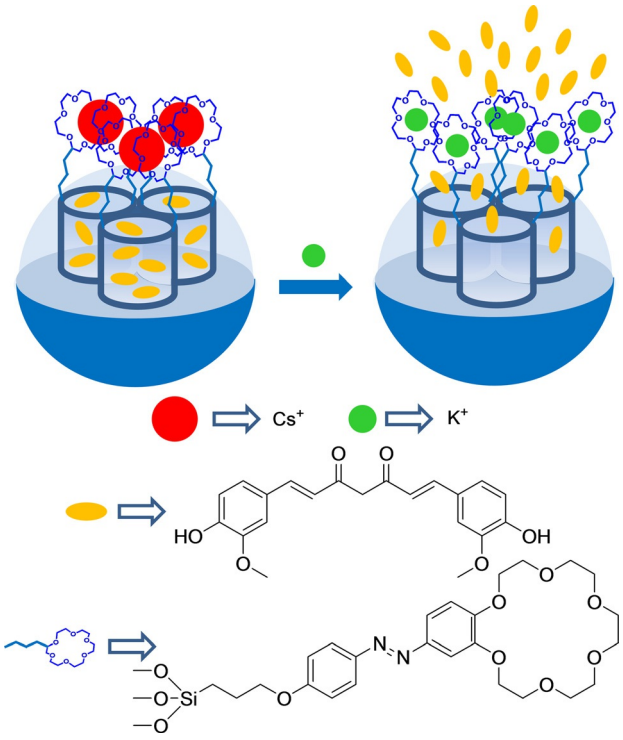


**Figure 11.** Nanometric silica mesoporous support loaded with curcumin and capped with $Cs^{+}$-18-crown-6 complexes for the detection of $K^{+}$ cations.

ticles were finally capped upon the addition of the $Cs^{+}$ cation, which formed sandwich complexes with the grafted 18-crown-6 moieties. The systems showed a zero release until the $K^{+}$ cation was added, which induced the release of the entrapped curcumin. The uncapping protocol was due to the $Cs^{+}$ exchange, owing to the formation of 1:1 macrocycle-$K^{+}$ complexes with a higher stability constant (see Figure 11). However the authors did not specifically use this system to sense applications, and no opening studies of macrocycle-capped nanoparticles with other metal cations were carried out. Nevertheless this study suggested the potential use of macrocycle-capped SMSs for sensing specific metal cations.

Metal-ion-dependent catalytic nucleic acids (DNAzymes) were used as caps by Willner et al. to prepare gated SMSs, which were selectively opened in the presence of cations $Mg^{2+}$ and $UO_2^{2+}$ (see Figure 12).[27] To prepare the $Mg^{2+}$-selective capped material, mesoporous silica nanoparticles were selected as an inorganic scaffold. In a first step, nanoparticles were functionalized with aminopropyl moieties. Then the amino groups reacted with a crosslinker agent, which yielded maleimide moieties on the external surface. Afterward, a thiolated ribonuclease, containing two complementary single-stranded DNA sequences (5′-HS-$(CH_2)_6$-CAG TGA ATT rAGG ACA TAG AAG AAG AAG-3′) of $Mg^{2+}$-dependent DNAzyme, was linked. In order to prepare the final sensing material, the pores were loaded with methylene blue and were then capped by the addition of the $Mg^{2+}$-dependent DNAzyme sequence 5′-CTT CTT CTT CTA TGT CAG CGA TTC CGG AAC GGA CAC CCA TGT ATT CAC TG-3′, through hybridization with the previously linked DNA sequence. The same experimental procedure was used to prepare the $UO_2^{2+}$-selective capped material, but thionine was employed as the loading molecule instead of methylene blue, and the pores capped with the $UO_2^{2+}$-dependent DNAzyme sequence 5′-CTT CTT CTT CTA TGT CAG CCG GAA CGG CCT TGC AAT TCA CTG-3′. Aqueous suspensions at pH 7.2 of $Mg^{2+}$-selective capped nanoparticles showed negligible methylene blue release in the absence of $Mg^{2+}$, whereas remarkable dye release was observed in the presence of this cation. The observed release was ascribed to the coordination of a $Mg^{2+}$ cation with linked DNAzyme, which induced cleavage of caps. The optical response was highly selective since the other divalent cations tested ($Zn^{2+}$, $Pb^{2+}$, $Ca^{2+}$, $Sr^{2+}$, $Ba^{2+}$, $Cu^{2+}$, $Co^{2+}$, $Mn^{2+}$, $Ni^{2+}$, $Fe^{2+}$, $Hg^{2+}$) were unable to induce pore opening and subsequent dye release. The same behavior, but at pH 5.2,

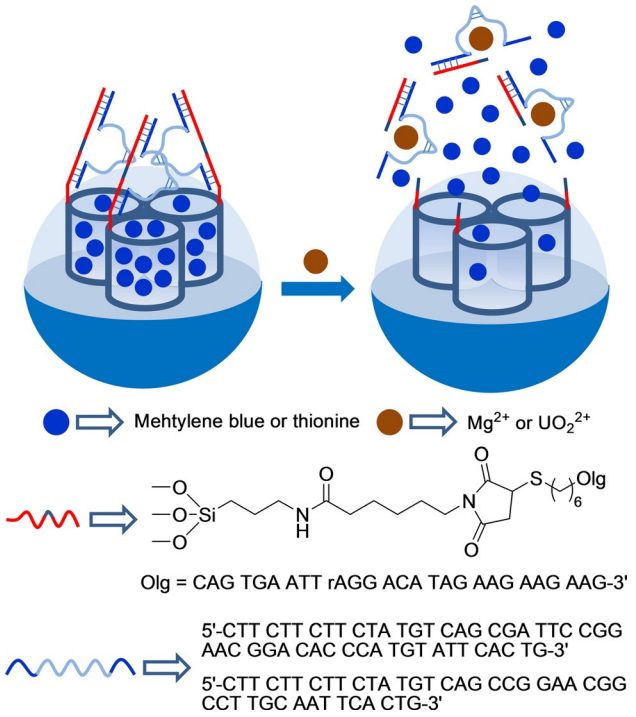


**Figure 12.** Nanometric silica mesoporous support loaded with methylene blue or methionine and capped with DNAzyme for the detection of $Mg^{2+}$ and $UO_2^{2+}$ cations.

and in the presence of cation $UO_2^{2+}$, was observed with the nanoparticles capped with the $UO_2^{2+}$-dependent DNAzyme sequence.

The same authors used DNAzymes as caps to prepare two materials which were opened in the presence of $Mg^{2+}$ and $Zn^{2+}$ cations.[28] Mesoporous silica nanoparticles were loaded with methylene blue or thionin and then functionalized with two different thiolated single strands of DNA (5′-CTT CTT CTT CTA TGT CAG CGA TCC GGA ACG GCA CCC ATG TTG TTG TTG-3′ for $Mg^{2+}$-dependent DNAzyme and 5′-CTT CTT CTT CTA TGT CTC CGA GCC GGT CGA AAT GTT GTT G-3′ for $Zn^{2+}$-dependent DNAzyme), using *N*-ε-maleimidicaproyl-oxosulfosuccinimide ester as crosslinker. The capped materials were able to release the entrapped dye in the presence of $Mg^{2+}$ and $Zn^{2+}$ cations, respectively, whereas other divalent metal cations ($Pb^{2+}$, $Ca^{2+}$, $Sr^{2+}$, $Ba^{2+}$, $Cu^{2+}$, $Co^{2+}$, $Mn^{2+}$, $Ni^{2+}$, $Fe^{2+}$, and $Hg^{2+}$) were unable to induce cargo delivery.

A similar approach was adopted by Tang and co-workers to prepare DNAzyme-capped mesoporous silica nanoparticles, which were selectively opened in the presence of cation $Pb^{2+}$.[29] Accordingly, silica mesoporous nanoparticles were selected as inorganic support and the external surface was functionalized with 3-glycidyloxipropyl trimethoxysilane. Then by an epoxy–amino reaction, $Pb^{2+}$-DNAzyme (5′-$NH_2$-TTT CAT CTC TTC TCC GAG CCG GTC GAA ATA GTG AGT-3′) was anchored to the surface, and the pores were loaded with glucose. Finally, the system was capped by the addition of a single-stranded DNA sequence (5′-ACT CAC TAT rAGG AAG AGA TG-3′) that hybridized with the grafted DNAzyme sequence (Figure 13). PBS (pH 7.4) suspensions of the capped nanoparticles showed negligible glucose release, whereas remarkable glucose delivery took place upon the addition of cation $Pb^{2+}$, measured by a personal glucometer. Cargo delivery was related to the cleavage of caps upon $Pb^{2+}$ coordination with the linked DNAzyme. The response was highly selective, and other cations tested ($Cu^{2+}$, $Co^{2+}$, $Cd^{2+}$, $Mg^{2+}$, $Zn^{2+}$, $Fe^{3+}$, $Ag^{+}$, and $Hg^{2+}$) were unable to induce glucose release.

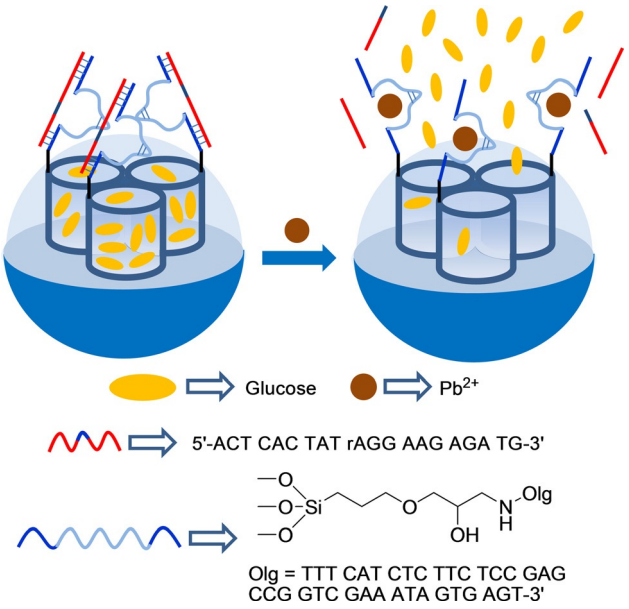


**Figure 13.** Nanometric silica mesoporous support loaded with glucose and capped with DNAzyme for the detection of $Pb^{2+}$ cations.

## 4 Sensing of Small Neutral Molecules

Lu and co-workers developed a gated SMS that was able to deliver an entrapped reporter using glucose as a trigger.[30] Mesoporous silica nanoparticles were selected as the inorganic scaffold, and their external surface was functionalized with prop-2-yn-1-yl(3-(triethoxyxilyl)propyl)carbamate. Following this functionalization, inhibitor D-(+)-glucosamine was grafted by a click chemistry reaction. Then pores were loaded with rhodamine B and capped by the addition of the glucose oxidase enzyme (GOx) through the formation of a complex with the grafted inhibitor (see Figure 14). PBS suspensions of the capped material showed negligible rhodamine B release, whereas the addition of glucose induced marked dye release. The observed release, which was proportional to the amount of glucose added, was the result of a displacement reaction of GOx from the pore outlets due to the formation of the corresponding glucose–GOx complex. The uncapping protocol was highly selective and the authors confirmed that other tested monosaccharides (i.e. fructose, mannose, and galactose) were unable to induce any rhodamine B release.

Villalonga and co-workers developed a new gated SMS in which an enzyme also acted as a cap (Figure 15). However in this case, the uncapping process was triggered by the product obtained by the enzyme's activity on glucose.[31] In their work, the authors loaded silica mesoporous nanoparticles with re-

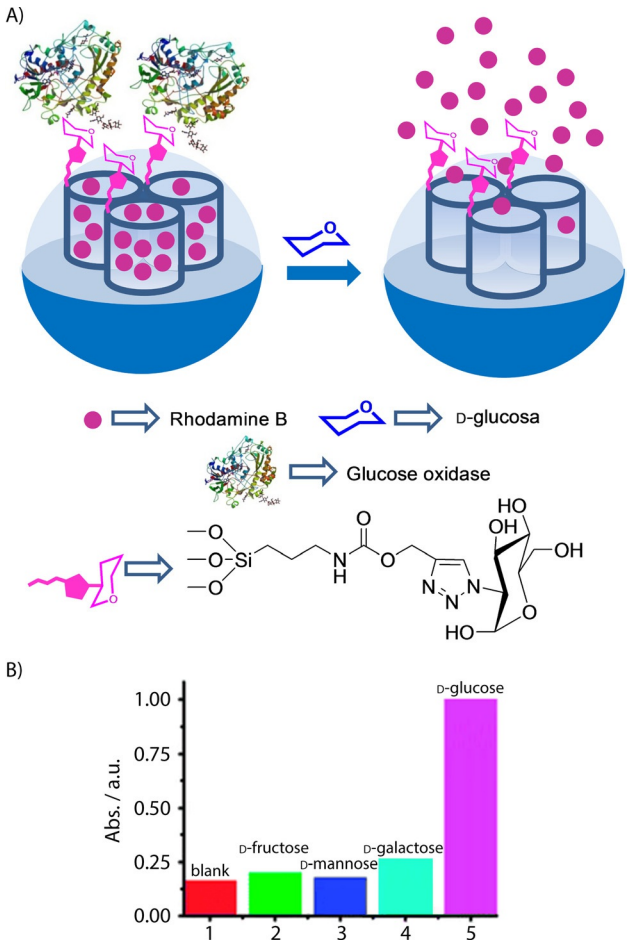


**Figure 14.** A) Nanometric silica mesoporous support loaded with rhodamine B and capped with glucose oxidase enzyme (GOx) for the detection of D-glucose. B) Selectivity release profile for the capped nanoparticles triggered by saccharides (1 mM glucose, 10 mM others). (Reproduced with permission from Ref. [30]. Copyright 2012, Royal Society of Chemistry).

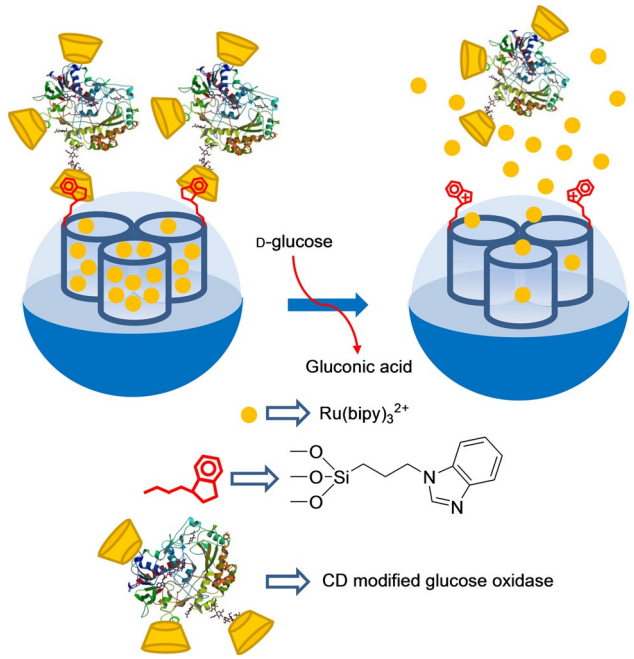


**Figure 15.** Nanometric silica mesoporous support loaded with $Ru(bipy)_3^{2+}$ and capped with cyclodextrin-modified glucose oxidase (CD-GOx) for the detection of D-glucose.

porter $Ru(bipy)_3^{2+}$ and functionalized the external surface with 3-iodopropyltrimethoxysilane, which was transformed into 1-propyl-1-*H*-benzimidazole moieties via a nucleophilic substitution reaction using benzimidazole. Mesopores were then capped with active cyclodextrin-modified glucose oxidase (CD-GOx) through the formation of an inclusion complex between the cyclodextrins and the propylbenzymidazole groups anchored to the solid support. In their study, these authors confirmed that dye delivery was induced when glucose was present in the solution due to the displacement of CD-GOx as a result of the CD-GOx-induced oxidation of glucose to gluconic acid, which induced the subsequent protonation of the benzimidazole groups. The response of the gated material was studied according to glucose concentration. The authors found a linear glucose response within the $1\times10^{-2}$–$1\times10^{-4}$ M range and a LOD of $1.5\times10^{-4}$ M which fell within the range of other glucose detection systems. The capped material was also tested in the presence of others saccharides, such as mannose, fructose, galactose, maltose, and saccharose, at the $1\times10^{-3}$ mol $L^{-1}$ concentration; however, no cargo delivery was observed.

In another work,[32] the same authors demonstrated that the gating mechanism and different effector ensembles can be integrated into a single system based on the use of Janus-type nanoparticles with opposing gold and mesoporous silica faces (see Figure 16). In particular, the porous network of the silica face was loaded with $Ru(bipy)_3^{2+}$ and the external surface was grafted with 3-(2-aminoethylamino)propyltrimethoxysilane. Aside from this, the AuNP side was functionalized with thiol-modified urease enzyme. Aqueous solutions (acetate buffer pH 5.0) of the Janus nanoparticles showed negligible dye release, because polyamines were protonated, and the molecular gate was closed. In the presence of urea, delivery of the entrapped complex was marked. This release resulted from the urease-catalyzed hydrolysis of urea into $CO_2$ and $NH_3$, which induced an increase in the local environment's pH. With this increase, polyamines became deprotonated, and gates subsequently opened.

Another gated system using Janus-type nanoparticles has been recently described.[33] The authors loaded the mesoporous silica face of Janus nanoparticles with $Ru(bipy)_3^{2+}$, and 3-iodopropyltrimethoxysilane was grafted onto the external surface. Through a nucleophilic substitution reaction, benzimidazole moieties were attached to anchored 3-iodopropyl residues, which resulted in 1-propyl-1*H*-benzimidazole groups. The pores were then blocked by the formation of inclusion complexes between β-CD moieties and the propylbenzimidazole groups. Thiol-modified esterase and GOx were covalently immobilized on the gold surface. Experimental results confirmed that the presence of either D-glucose or ethyl butyrate, or a combination of both, brought about a drop in pH locally through an enzyme-catalyzed substrate conversion into gluconic acid or butyric acid, which induced the opening of the

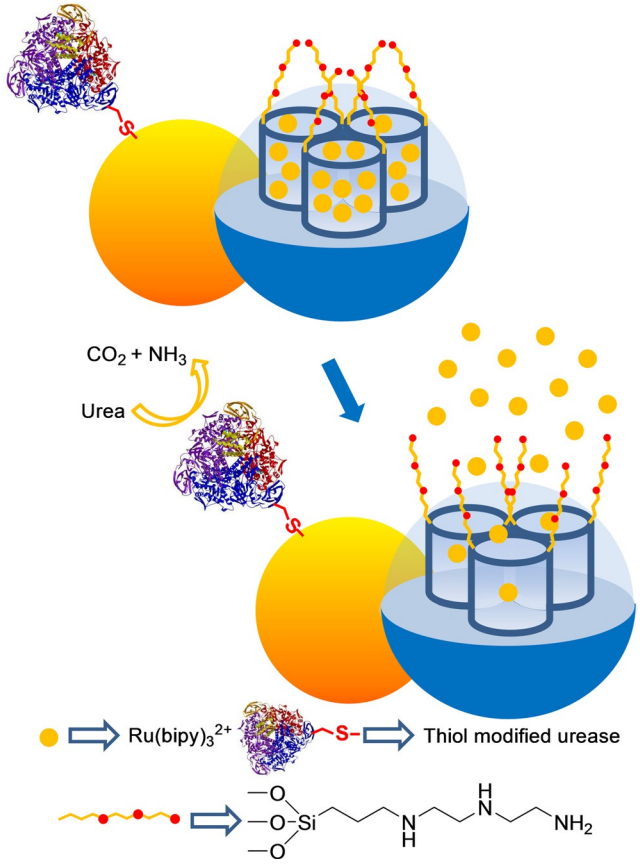


**Figure 16.** Janus gold–silica mesoporous nanoparticle support loaded with $Ru(bipy)_3^{2+}$ and capped with polyamines for the detection of urea.

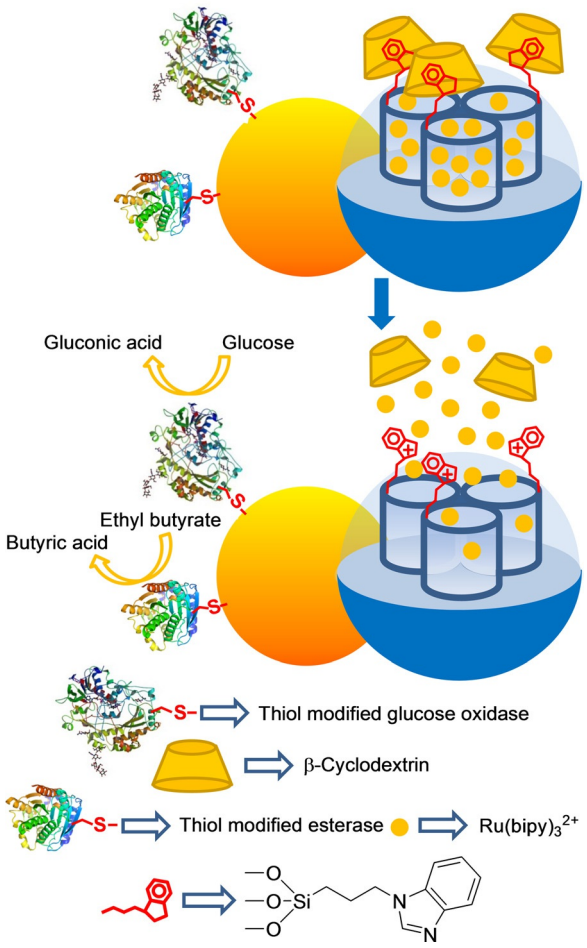


**Figure 17.** Janus gold–silica mesoporous nanoparticle support loaded with $Ru(bipy)_3^{2+}$ and capped with β-CD for the detection of D-glucose and ethyl butyrate.

β-CD-gated nanovalves and entrapped dye release (see Figure 17).

Kim and co-workers developed an SMS that was selectively opened in the presence of fructose and galactose. Mesoporous silica nanoparticles were grafted with amine moieties and coupled with *p*-dihydroxyborylbenzoic acid. Hybrid material was loaded with calcein, and the boronic acid units on the surface were indistinctly coordinated to α-, β-, or γ-CD (Figure 18). Fluorescence spectrometry measurements showed clear dye delivery in the presence of fructose and galactose, whereas no delivery for mannose or glucose occurred. The LODs for D-fructose or D-galactose were not determined. Probe uncapping was explained by the displacement of bulky cyclodextrins by the competitive interaction of monosaccharides with boronic acid moieties.[34] It is also worth mentioning that, despite not having been designed specifically for sensing purposes, other authors have developed selective glucose-responsive systems, and have used them for the glucose-induced release of insulin, which was related directly with the amount of glucose present in media.[35,36]

Martínez–Máñez et al[37] reported the design of a capped SMS for the selective chromo-fluorogenic detection of glutathione (GSH) in both pure water and human serum (see Figure 19). This system consisted of mesoporous silica nanoparticles, which were first loaded with safranin O as a reporter. Then the external surface was functionalized with (3-mercapto-

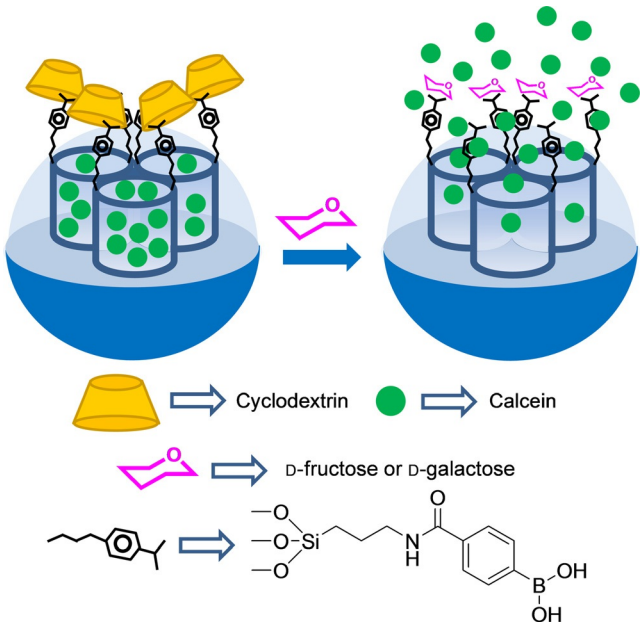


**Figure 18.** Nanometric silica mesoporous support loaded with calcein and capped with α-, β- or γ-CD for the detection of fructose or galactose.

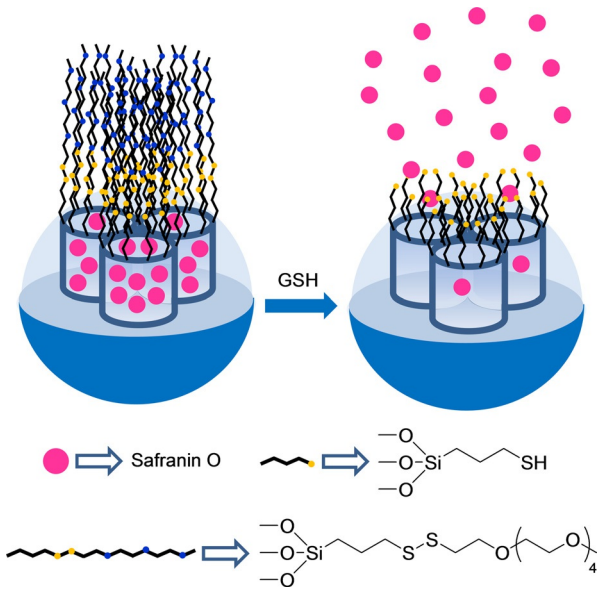


**Figure 19.** Nanometric silica mesoporous support loaded with safranin O and capped with poly(ethylene glycol) for the detection of glutathione (GSH).

propyl)trimethoxysilane, and the thiol-functionalized solid was further reacted with 2,2′-dipyridyl disulfide. The final sensing solid was obtained by a reaction with O-(2-mercaptoethyl)-O′-methyl-hexa(ethyleneglycol). The signaling mechanism was based on a selective GSH-induced reduction of the disulfide bond, which resulted in pore opening and entrapped dye release. A correlation between the delivered dye and the amount of glutathione was observed in the release experiments. These authors obtained a LOD of 0.1 μM for glutathione in both pure water and human serum. The gated system was demonstrated to be highly selective for glutathione against similar sulfur-containing derivatives (cysteine, homocysteine, *S*-methyl cysteine, $HS^-$), anions ($F^-$, $Br^-$, $Cl^-$, $I^-$, $CN^-$, $OH^-$, $HPO_4^-$, $AcO^-$, citrate, $N_3^-$, $NO_3^-$, $SO_3^{2-}$, $SO_4^{2-}$, and $S_2O_4^{2-}$), and oxidants ($H_2O_2$).

The same group reported a family of capped SMS for the fluorimetric sensing of nitroaromatic explosives (Figure 20 A).[38] In a first example, the authors designed an SMS loaded with $Ru(bipy)_3^{2+}$ as a fluorophore and functionalized on the surface with 3-(azidopropyl) triethoxysilane groups. Afterward, a suitable pyrene derivative was attached to azido moieties by a copper(I)-catalyzed Huisgen azide/alkyne 1,3-dipolar cycloaddition click reaction, which led to the formation of a 1,2,3-triazole heterocycle and yielded the final sensing material. Pores were blocked by the presence of a dense network of bulky pyrene moieties on the outer surface. As a result, dye delivery in acetonitrile was inhibited. Presence of nitroaromatic explosives 2,4,6-trinitrophenylmethylnitramine (Tetryl) and 2,4,6-trinitrotoluene (TNT) induced the formation of pyrene–nitroaromatic complexes, which pushed apart the bulky pyrene from pore voids to thus unblock pores, and allowed dye release. LODs of 1.4 and 11.4 ppm for Tetryl and TNT, respectively, were calculated by fluorogenic titration curves. In addition, a LOD was also calculated from the nitroaromatic-induced quenching of

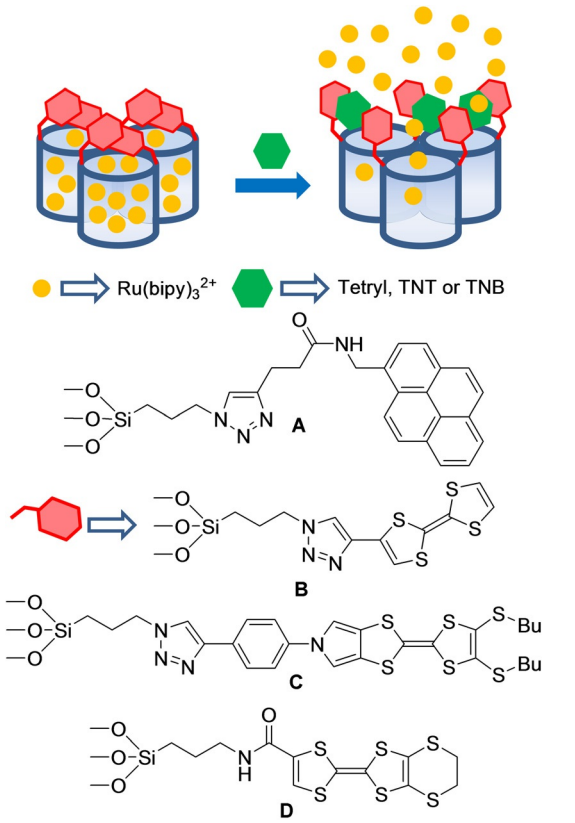


**Figure 20.** Micrometric silica mesoporous support loaded with $Ru(bipy)_3^{2+}$ and capped with pyrene or tetrathiafulvalene (TTF) derivatives for the detection of nitroaromatic explosives.

pyrene emission. With this procedure, LODs of 8.6 and 9.1 ppm for Tetryl and TNT were respectively obtained. Finally, selectivity studies performed in the presence of other aromatic derivatives (e.g. 2,4-dinitrotoluene, *N*-methylaniline, 2-nitrotoluene, and nitrobenzene), nonaromatic explosives (e.g. hexahydro-1,3,5-trinitro-1,3,5-triazine and pentaerythritol tetranitrate), methylene blue, and naphthalene were carried out. These studies showed that 2,4-dinitrotoluene (DNT) was also able to induce partial entrapped-fluorophore release, but to a lesser extent.

In a later work,[39] the same authors reported the use of a tetrathiafulvalene (TTF)-capped SMS for the detection of certain nitroaromatic explosives (Figure 20 B). The SMS was loaded with $Ru(bipy)_3^{2+}$ as the reporter and the TTF derivative was anchored to the surface by a copper(I)-catalyzed Huisgen azide/alkyne 1,3-dipolar cycloaddition click reaction. Presence of a dense network of TTF units around pores inhibited dye delivery. Release studies into acetonitrile revealed that presence of Tetryl, TNT, and to a lesser extent of 1,3,5-trinitrobenzene (TNB), induced pore opening and dye release. From UV-vis titration studies, LODs of 28 μM (8 ppm) and 66 μM (15 ppm) for Tetryl and TNT, respectively, were calculated. With fluorescence measurements, LODs of 3.5 μM (1 ppm) and 26 μM (6 ppm) for Tetryl and TNT, respectively, were found.

These authors also reported a similar TTF-capped SMS, but in this case they used different TTF derivatives of varying sizes

and shapes, and incorporated different numbers of sulfur atoms (Figure 20C,D).[40] In all cases, sensing supports were loaded with the $Ru(bipy)_3^{2+}$ reporter. The slight differences found in the chemical structures of TTF-capping molecules resulted in different responses of solids. Of all the explosives tested, only Tetryl, TNT, and TNB were capable of inducing, to some extent, the dye release from sensing materials. By using color or emission measurements, the LODs within the 1–10 ppm range for the detection of these explosives were calculated. By using one of these TTF-capped SMSs, the authors were able to detect low levels of Tetryl in soil samples with good results.

Capped silica mesoporous supports have also been used to detect nerve agent simulants (Figure 21).[41] Nerve agents (such as Sarin, Soman, and Tabun) are highly toxic organophosphorous compounds that have severe effects on human health and have been used in terrorist attacks. Given the high toxicity of these chemicals, simulants diethyl chlorophosphate (DCP), diisopropylfluorophosphate (DFP), and diethyl cyanophosphate (DCNP), which present similar reactivity to nerve agents, but are much less toxic, were used in this work. The sensing system was based on an SMS loaded with $Ru(bipy)_3^{2+}$ and capped with the bis(2-hydroxyethyl)aminopropyltriethoxysilane (HET) groups. These HET moieties formed a thick hydrogen-bonding network around pore outlets, especially in aprotic solvents (e.g. acetonitrile) and inhibited dye delivery. These authors observed that addition of nerve agent simulants induced pore opening, which resulted in selective entrapped dye release. This release was attributed to the reaction between the nerve agent simulants and –OH groups in HET, which induced the rupture of the dense hydrogen-bonding network to result in dye release. Simple chromogenic titrations allowed the detection of DCP down to about 15 ppm, whereas the use of fluorimetric procedures permitted the detection of DCP at concentrations as low as 0.1 ppm. Similar LODs were obtained for DFP and DCNP, whereas other tested organophosphorus compounds induced no response. This material was also used to detect nerve agent mimics in the gas phase with good results.

The design of gated systems involving biomolecules as capping agents for the detection of small molecules has also been recently explored. One of the first works in this area used a polyclonal antibody for capping pores. In this first work, an antibody for sulfathiazole was selected (see Figure 22A).[42] Specifically, the authors loaded the pores of the SMS with reporter $Ru(bipy)_3^{2+}$ and anchored the silane derivative 4-(4-aminobenzenesulfonylamino)benzoic acid on the pore outlets of the inorganic support. Finally the material was capped with a polyclonal antibody for sulfathiazole, which also showed good affinity for the anchored molecule. The authors found that the ruthenium complex was released when the antigen for the capping antibody (e.g. sulfathiazole) was present in the solution. A LOD of about 100 ppb for sulfathiazole was determined. The system was highly selective, and dye delivery was observed only for sulfatiazole, whereas it remained closed in the presence of a family of related compounds.

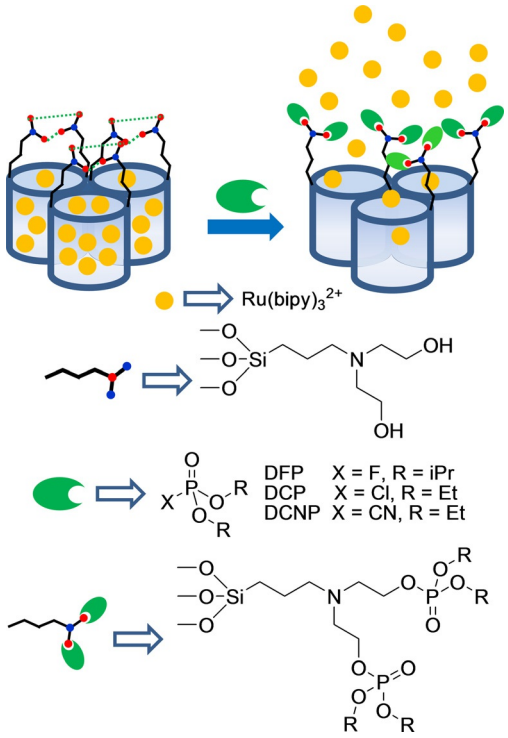


**Figure 21.** Micrometric silica mesoporous support loaded with $Ru(bipy)_3^{2+}$ and capped with hydroxyamino groups for the detection of nerve agent simulants.

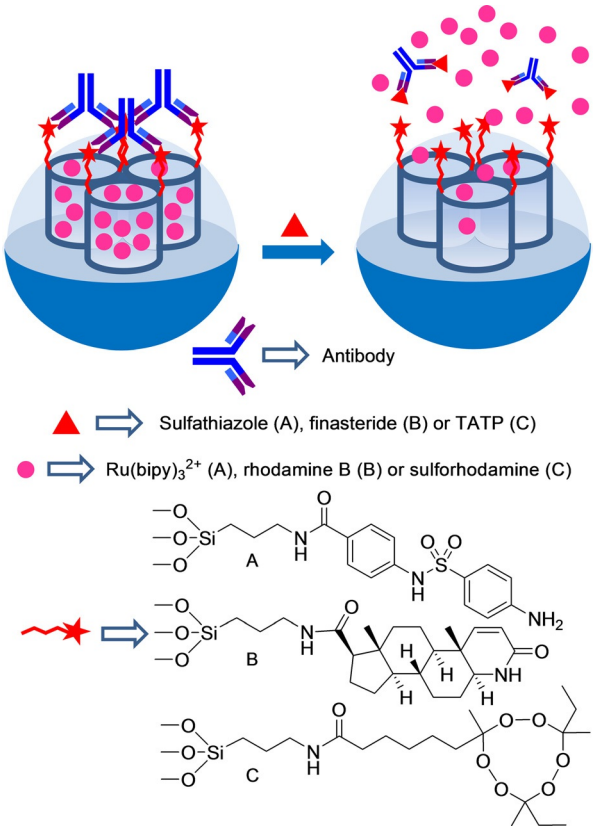


**Figure 22.** Nanometric silica mesoporous support loaded with $Ru(bipy)_3^{2+}$ and capped with different antibodies for the detection of sulfathiazole, finasteride and triacetone triperoxide (TATP).

Martínez–Máñez et al.[43] further developed an antibody-capped SMS for the selective detection of finasteride with a similar approach (see Figure 22B). In this case, the mesoporous support was loaded with rhodamine B and functionalized with *N*-(*tert*-butyl)-3-oxo-(5a,17b)-4-aza-androst-1-ene-17-carboxamide groups (a similar molecule to finasteride) on the external surface. Addition of polyclonal antibodies for finasteride induced capping of pores due to the interaction with the anchored hapten-like derivative. Addition of finasteride to water suspensions of the antibody-capped material led to the antibody being displaced, pores being uncapped, and the entrapped dye being released. The amount of delivered dye was found to be proportional to the finasteride concentration, and a typical noncompetitive immunoassay response curve with a LOD of 20 ppb was displayed. Selectivity studies showed that only finasteride, among all the other steroids (testosterone, metenoloneand 16-β-hydroxystanozolol), was able to induce a significant uncapping process. The material was isolated and stored to be finally tested to detect finasteride in spiked urine samples. Recovery ranges from 94% to 118% were observed.

By following a similar protocol, a new antibody-gated dye-delivery system for the detection of peroxide-based explosive triacetone triperoxide (TATP) by test-strip assays was developed (see Figure 22C).[44] In this work, an SMS in the form of nanoparticles was loaded with dye sulforhodamine B. Then the external surface was functionalized with an appropriate hapten-like molecule, and the system was capped using a TATP-selective polyclonal antibody. The uncapping of pores with the subsequent dye delivery in the presence of TATP was remarkable and highly selective in PBS (pH 7.4). With this protocol, TATP was detected at concentrations as low as 12.5 ppb. The authors also demonstrated that the capped SMS can be integrated into a lateral-flow assay. Using this latter procedure, a LOD of 15 ppb for TATP was determined. The system proved highly selective. Common explosives, like TNT, hexogen, nitropenta, octogen, nitroguanidine, and hexamethylene triperoxide diamine, were unable to uncap pores.

A probe that also employed antibodies, but based on a different configuration, has been recently developed by Zhang et al. for the detection of biotoxin brevetoxin B (PbTx-2), a neurotoxin produced by algae that can cause intoxication (see Figure 23).[45] These authors used mesoporous silica nanoparticles of 150 nm, which were first functionalized with aminopropyl groups. Afterward, an antibody for brevetoxin B was attached to the amino moieties by using glutaraldehyde as a linker. In order to avoid the detachment of the linked antibody, the formed imine bonds were further reduced by the addition of sodium cyanoborohydride. Finally, the pores of the nanoparticles were loaded with methylene blue and capped upon the addition of aminated polystyrene spheres with a diameter of 25 nm. The capping protocol was carried out in PBS at pH 6.5. At this pH, strong electrostatic interactions occurred between the grafted antibody, which was negatively charged, and the aminated polystyrene spheres, which were positively charged. Addition of brevetoxin B induced a remarkable methylene blue release, detected by voltammetry due to the selective interaction of this toxin with the grafted antibody and the

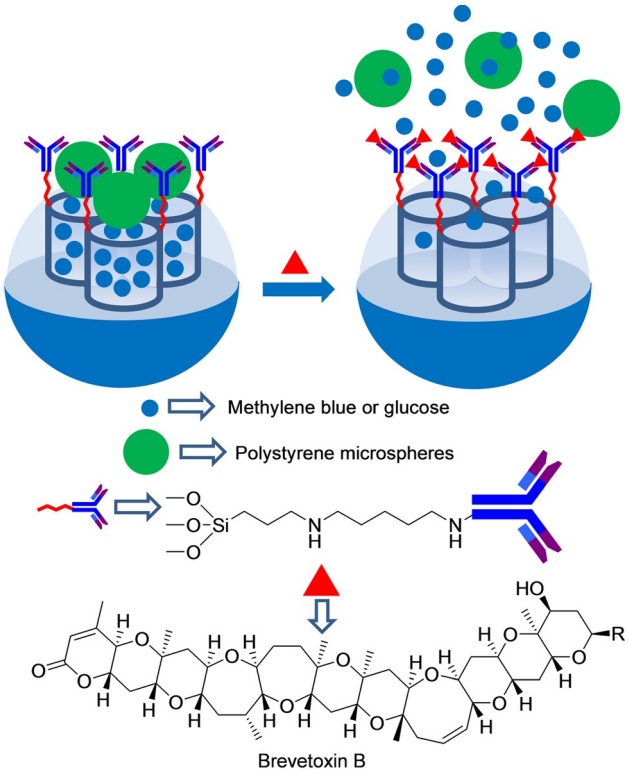


**Figure 23.** Nanometric silica mesoporous support loaded with methylene blue or glucose and capped with antibody–polystyrene microspheres for the detection of brevetoxin B.

subsequent displacement of the polystyrene spheres from the surface of the nanoparticles. Linear dependence from 10 pg mL$^{-1}$ to 3.5 ng mL$^{-1}$ between the peak current and the PbTx-2 concentration was observed. These authors also calculated a LOD of 6 pg mL$^{-1}$ for PbTx-2, which was significantly lower than that of a commercially available PbTx-2 enzyme-linked immunosorbent assay (ELISA) kit. The capped system showed high cross-reactivity for PbTx-1 and PbTx-3, explained by the non-specificity of the anti-PbTx-2 antibody used for these analytes. The system responded to neither okadaic acid, aflatoxin B1, and microcystin-LR, nor the presence of several possible components in seawater, including $Na^+$, $Ca^{2+}$, $Mg^{2+}$, $Cl^-$, $SO_4^{2-}$, $HCO_3^-$, and $F^-$. The sensing system was tested for the detection of PbTx-2 in different food samples. In another work done in 2014, the same authors applied a similar antibody-gated design to detect PbTx-2 coupled with a portable personal glucometer.[46] The authors loaded a magnetic mesoporous $NiCo_2O_4$ nanostructure with glucose, and pores were capped by adopting a similar protocol to that described above. In the presence of PbTx-2, gated nanoparticles were uncapped to release glucose, which was quantitatively determined by a simple glucometer. This particular system displayed a signal that was proportional to PbTx-2 up to a concentration of about 20 ng mL$^{-1}$. A LOD of 0.01 ng mL$^{-1}$ for PbTx-2 was calculated. The authors also confirmed the potential use of capped nanoparticles to detect PbTx-2 in real samples.

Tang et al.[47] used a similar approach to detect the mycotoxin aflatoxin $B_1$ ($AFB_1$). For this purpose, the pores of polyethy-

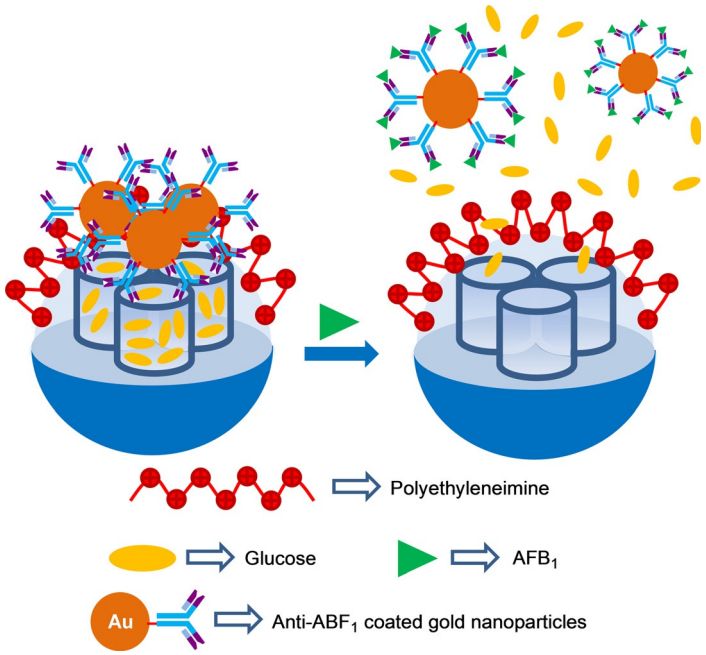


**Figure 24.** Nanometric silica mesoporous support loaded with glucose and capped with antibody–AuNPs for the detection of aflatoxin $B_1$ ($AFB_1$).

leneimine-coated silica mesoporous nanoparticles were loaded with glucose (Figure 24). Afterward, pores were capped upon the addition of AuNPs functionalized with antibodies for $AFB_1$ (through electrostatic interactions between the positively charged polyethyleneimine shell and the negatively charged antibodies). The proper working of the final gated material was assessed by a personal glucometer. Buffered suspensions (pH 7.3) of capped nanoparticles showed no signal, whereas marked glucose release was observed in the presence of $AFB_1$. This release was ascribed to the coordination of $AFB_1$ with the antibodies and the subsequent detachment of AuNPs. Linear dependence from 0.01 ppb to 15 ppb between the personal glucometer readout and the $AFB_1$ concentration was observed. These authors calculated a LOD of 5 ppt for $AFB_1$.

The same authors presented a new fluorescence immunoassay to detect $AFB_1$.[48] In order to build the designed immunosensing probe, mannose-terminated silanes were covalently attached to the external SMS surface. Subsequently, pores were loaded with rhodamine B and capped with biotinylated concanavalin A (Con A) via multivalent carbohydrate–protein interactions. Biotinylated Con A and biotinylated anti-$AFB_1$ were conjugated with streptavidin. At the same time, AuNPs were functionalized with invertase and with a bovine serum albumin (BSA)–$AFB_1$ conjugate. When target $AFB_1$ was present, a competitive immunoreaction was carried out for the immobilized anti-$AFB_1$ antibody on the SMS between the target analyte ($AFB_1$) and the labeled $AFB_1$–BSA on AuNP. Therefore, the amount of functionalized AuNPs on SMSs decreased when the target AFB1 concentration increased in the sample. Upon sucrose addition, an invertase on AuNP hydrolyzed sucrose into glucose and fructose. The generated glucose competed with mannose for Con A coordination and unblocked pores, and released the entrapped dye (see Figure 25). The release experiments of the immunosensing probe in Tris buffer (pH 6) in the presence of sucrose showed linear dependence between the fluorescence signal and the $AFB_1$ concentration within the 10 pg mL$^{-1}$–5 ng mL$^{-1}$ range. A LOD of 8 pg mL$^{-1}$ (8 ppt) was calculated for $AFB_1$. These authors also tested the system's response in the presence of $Zn^{2+}$, $Na^+$, $K^+$, $Cl^-$, $HCO_3^-$, $NO_3^-$, collagens, mucins, thyroid-stimulating hormone, and α-fetoprotein. The results showed that inorganic ions did not interfere with $AFB_1$ detection. However, presence of glycoproteins in the sample increased fluorescence intensity to some extent.

Wen and co-workers prepared AuNP-aptamer-capped SMSs for the detection of adenosine (Figure 26).[49] For this purpose, mesoporous silica nanoparticles were functionalized with 3-aminopropyl moieties and amino groups were transformed into carboxylic acids by a reaction with succinic anhydride. Then the ssDNA sequence 3′-$NH_2C_6$-TCT CTT GGA CCC CCT-5′ was

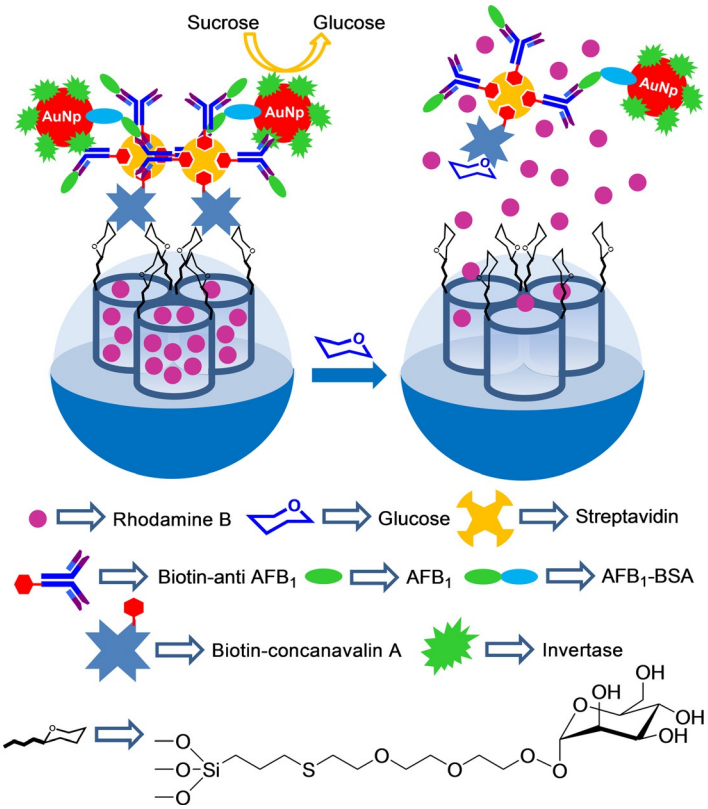


**Figure 25.** Nanometric silica mesoporous support loaded with rhodamine B and capped with functionalized AuNPs for the detection of aflatoxin $B_1$ ($AFB_1$).

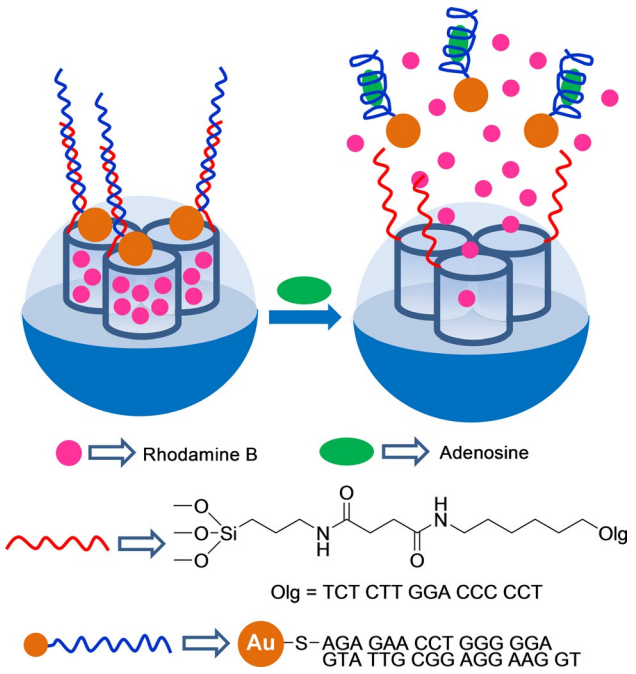


**Figure 26.** Nanometric silica mesoporous support loaded with rhodamine B and capped with adenosine aptamer AuNPs for the detection of adenosine.

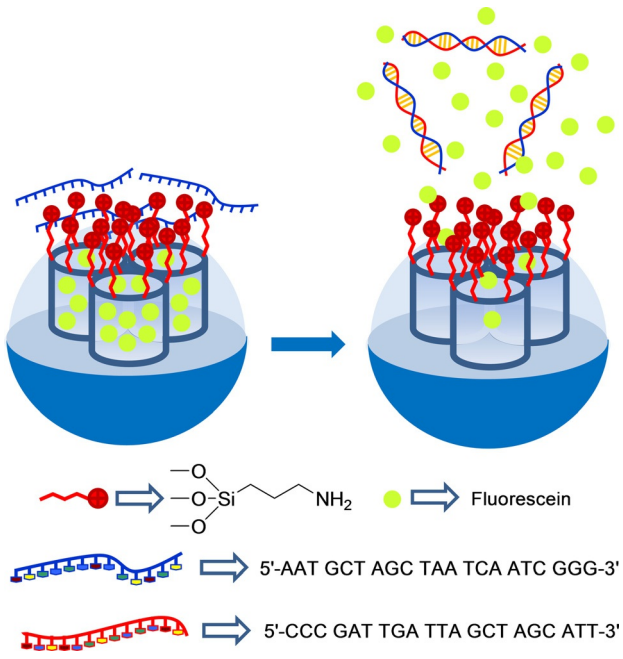


**Figure 27.** Nanometric silica mesoporous support loaded with fluorescein and capped with oligonucleotide for the detection of the complementary strand.

grafted on the outer surface by an amidation reaction. At this point, pores were loaded with rhodamine B. Finally, pores were capped with AuNPs functionalized with a complementary aptamer for adenosine (e.g. AuNP-S-AGA GAA CCT GGG GGA GTA TTG CGG AGG AAG GT-3′). Aqueous suspensions of capped nanoparticles showed negligible dye release. However, addition of adenosine induced pore opening and entrapped rhodamine B release due to the formation of aptamer–adenosine complexes that detached AuNPs from the SMS surface. The observed response was selective, and the authors found that addition of cytidine, guanosine, and uridine induced negligible rhodamine B delivery.

## 5 Sensing of Biomolecules

A first example of a capping–uncapping protocol for the detection of biomolecules, in particular a certain oligonucleotide, was reported by Martínez–Máñez et al (Figure 27).[50] The system was based on an SMS in the form of nanoparticles loaded with fluorescein and functionalized with (3-aminopropyl)triethoxysilane on the outer surface. Oligonucleotide 5′-AAT GCT AGC TAA TCA ATC GGG-3′ was used to cap pores via electrostatic interactions with the anchored amines partially protonated in water at a neutral pH. These authors demonstrated that delivery of dye from the solid at pH 7.5 was selectively triggered in the presence of the complementary single strand of the capping oligonucleotide due to the hybridization of both single oligonucleotide sequences with the concomitant cargo release. They also tested dye delivery in the presence of other oligonucleotides with a single or two-base mismatch sequence(s), but delivery was poor in these cases.

By taking the system one step forward, these authors designed a similar capped material to detect genomic DNA (Figure 28).[51] For this purpose, an SMS, also in the form of nanoparticles, was loaded with rhodamine B and functionalized with (3-aminopropyl)triethoxysilane on the external surface. As the capping oligonucleotide, a highly conserved sequence in the *Mycoplasma* genome, which corresponds to a fragment of the 16S ribosomal RNA subunit, was used (e.g. 5′-GGG AGC AAA CAG GAT TAG ATA CCC T-3′). The system remained closed until the genomic DNA of *Mycoplasma fermentans* was added, which had been previously dehybridized by thermal treatment. The capped SMS was unable to deliver the cargo in the presence of genomic DNA from other bacteria, such as *Candida albicans* or *Legionella pneumophilla*. A LOD as low as about 50 DNA copies $\mu L^{-1}$ was determined. Capped nanoparticles were used to detect *Mycoplasma* contamination in real contaminated cell culture media without applying PCR techniques.

In a more recent work, the same authors developed a similar system to detect genomic DNA. In this case, they used nanoparticles loaded with rhodamine B and capped with covalently attached DNA (see Figure 29).[52] Two single-stranded oligonucleotides were selected for the gating mechanism: 1) a short DNA sequence ($NH_2$-$(CH_2)_6$-5′-GAC TAC GAC GGT ATC-3′), which was covalently anchored to the SMS via the formation of urea bonds and 2) a single-stranded oligonucleotide selective for *Mycoplasma* (e.g. 5′-AAG CGT GGG GAG CAA ACA GGA TTA GAT ACC CTG GTA GTC-3′). The probe was able to detect *Mycoplasma fermentas* genomic DNA at a concentration as low as 70 DNA copies $\mu L^{-1}$. The authors also found that *Candida albicans* and *Legionella pneumophilla* genomic DNA were unable to induce dye release.

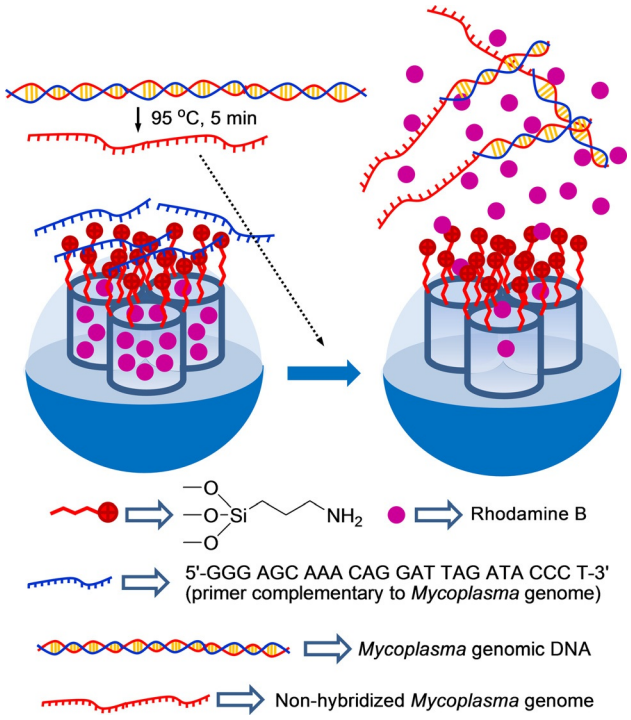


**Figure 28.** Nanometric silica mesoporous support loaded with rhodamine B and capped with a single-stranded oligonucleotide for the detection *Mycoplasma fermentans* genomic DNA.

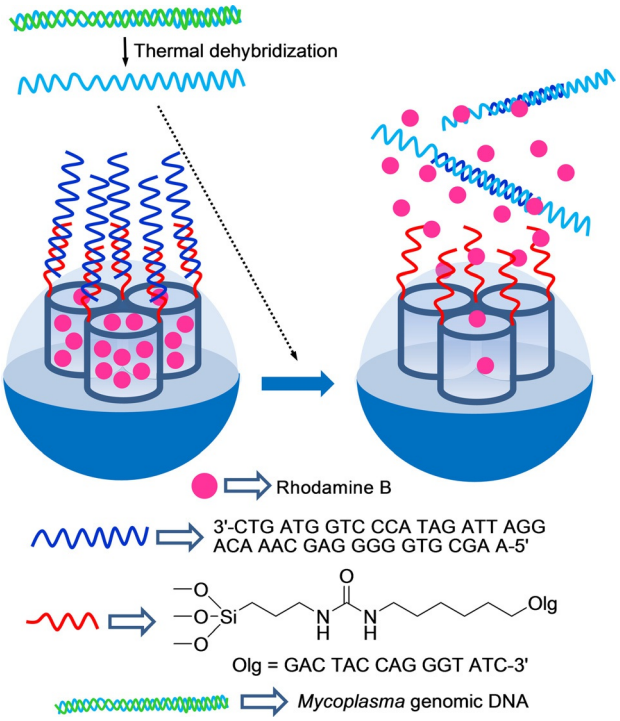


**Figure 29.** Nanometric silica mesoporous support loaded with rhodamine B and capped with covalently anchored oligonucleotides for the detection *Mycoplasma fermentans* genomic DNA.

He, Wang, and co-workers combined the catalytic properties of platinum nanoparticles (PtNPs) and capped mesoporous silica to develop a colorimetric detection system for oligonucleotides (see Figure 30).[53] For this purpose, and as an inorganic scaffold, PtNPs were synthesized and then coated with a mesoporous silica shell. In order to prepare the final gated material, the external silica shell was functionalized with aminopropyl moieties, and pores were capped through electrostatic interactions with the single oligonucleotide strand 5′-TCT TTC CTT GAT TTT CTT CCT TTT GTT CAC-3′, which contained a mutation of gene BRCA1, which is related to breast cancer. Buffered (acetate, pH 4.7) suspensions of capped nanoparticles in the presence of 3,3′,5,5′-tetramethylbenzidine (TMB) remained colorless because the molecules of the indicator were unable to access the platinum core. However, in the presence of the complementary strand, a clear blue color developed due to the displacement of the capping oligonucleotide and the Pt-induced catalytic oxidation of TMB. The system's response time was very short (between 3 and 10 min), and the LOD was calculated to be 3 nM. Aside from this, other strands with one, two, or three mismatched bases induced negligible color changes.

The groups of Martínez–Máñez[54] and Yang[55] simultaneously developed aptamer-gated SMSs based on a similar synthetic approach, but with different analytical techniques, to detect thrombin. Martínez-Máñez et al. used mesoporous silica nanoparticles loaded with dye rhodamine B (see Figure 31), while Yang's system consisted of $Fe_3O_4$ magnetic nanoparticles coated with a mesoporous silica shell loaded with the $Ru(bipy)_3^{2+}$ complex. In both cases, external SMS surfaces were

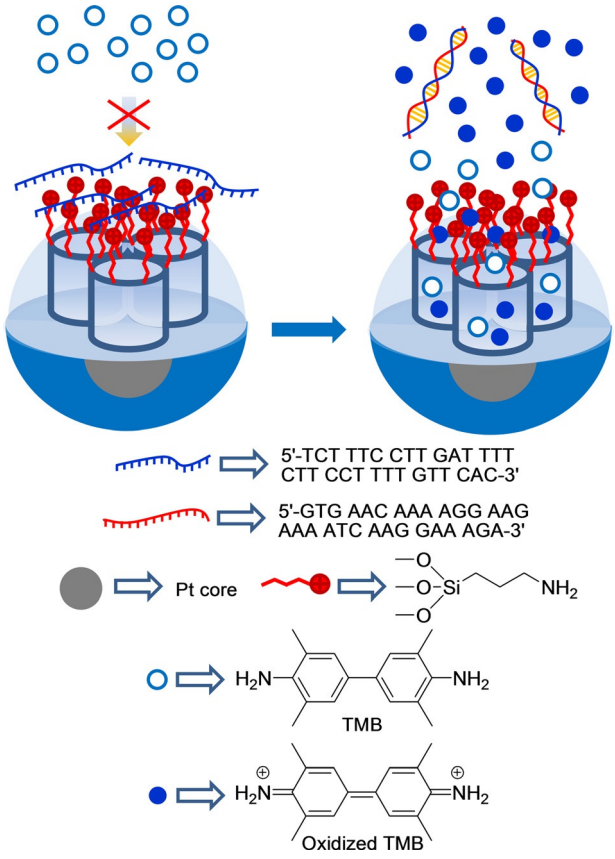


**Figure 30.** Nanometric core-shell platinum–silica mesoporous support capped with oligonucleotide for the detection of the complementary strand.

grafted with 3-aminopropyltriethoxysilane, and the 15-mer thrombin-binding aptamer 5′-TTT TTTGGTTGGTGTGGT TGG-3′ (TBA) was used as a gatekeeper. The aptamer was absorbed on the surface through electrostatic interactions with the positively charged amines on SMS surfaces. In the presence of α-thrombin, the TBA aptamer was displaced from the surface, due to the formation of TBA–protein complexes, and the entrapped reporter was delivered. Martínez–Máñez et al. detected presence of thrombin by measuring the fluorescence emission of the rhodamine B dye in the solution. These authors tested their system successfully in simulated human blood plasma and achieved a LOD of 2 nM, and a LOD of 4 nM in PBS buffer with 10% human serum. Yang et al. studied the presence of thrombin by detecting the electrochemiluminescence of the $Ru(bipy)_3^{2+}$ reporter. This allowed them to calculate a LOD of 0.5 pM in Tris-HCl buffer. Martínez–Máñez et al. found that a mixture of other nonexclusive binding proteins, such as ovalbumin and BSA, was unable to induce the uncapping of pores.

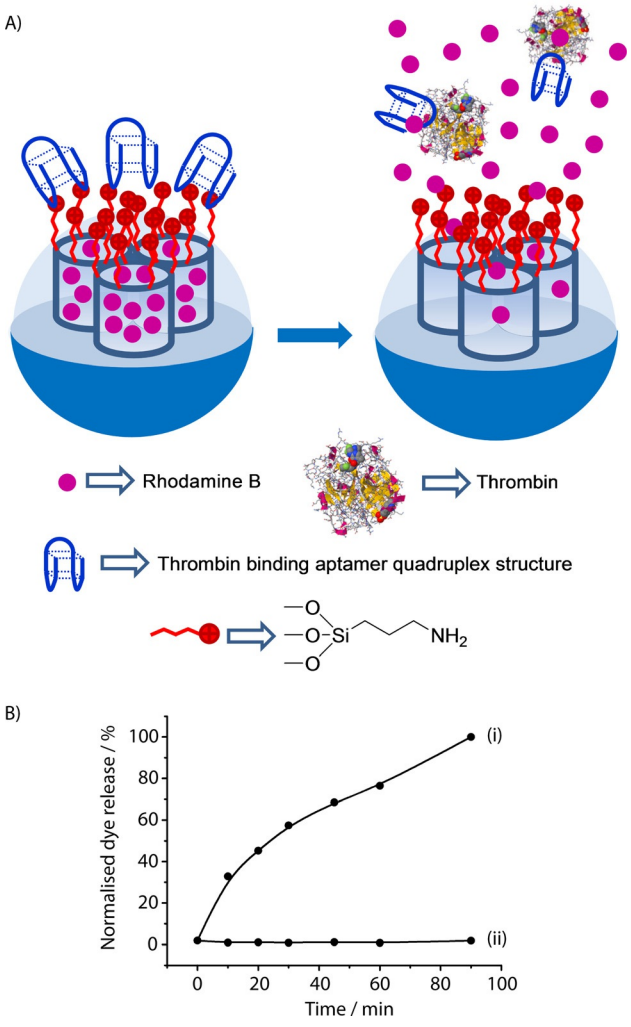


**Figure 31.** A) Nanometric silica mesoporous support loaded with rhodamine B and capped with thrombin binding aptamer for the detection of thrombin. B) Release profile of rhodamine B from the capped solid in the presence (i) and in the absence (ii) of thrombin in simulated human blood plasma. (Reproduced with permission from Ref. [54]. Copyright 2013, Royal Society of Chemistry).

Similarly, Yang et al demonstrated that BSA, lysozyme, and GOx possessed negligible uncapping capacity.

DNA-capped mesoporous silica nanoparticles have also been used for the optical and electrochemical detection of the glycoprotein enzyme prostate-specific antigen (PSA).[56] The SMS was functionalized with aminopropyl moieties, and pores were loaded with methylene blue. Finally, pores were capped upon the addition of a single DNA strand (5′-GTA ATC CTC AGC AAC CTC AGC-3′) by electrostatic interactions with the positively charged nanoparticle surface. The uncapping protocol was related with the use of two antibodies capable of coordinating PSA, which were labeled with two ssDNA fragments (DNA1: 5′-GCT GAG GTT ATC AAG ACT TTT TTT ATC ACA TCA GGC TCT AGC GTA TGC TAT TG-SH-3′ and DNA2: 5′-SH-TAC GTC CAG AAC TTT ACC AAA CCA CAC CCT TTT TTT GTC TTG GCT GAG GAT-3′), which were complementary to that used for capping mesoporous nanoparticles. In the presence of both DNA-labeled antibodies and PSA, a proximate complex was formed and was able to hybridize with the ssDNA used as the cap, which resulted in methylene blue release (see Figure 32). Cargo release was measured through fluorescence or differential pulse voltammetry. PSA was sensitively detected with a linear range from 0.002 to 100 ng mL$^{-1}$, and a LOD of 1.3 pg ml$^{-1}$ was determined. No interference was observed in the detection of PSA when the carcinoembryonic antigen (CEA) was present in the solution.

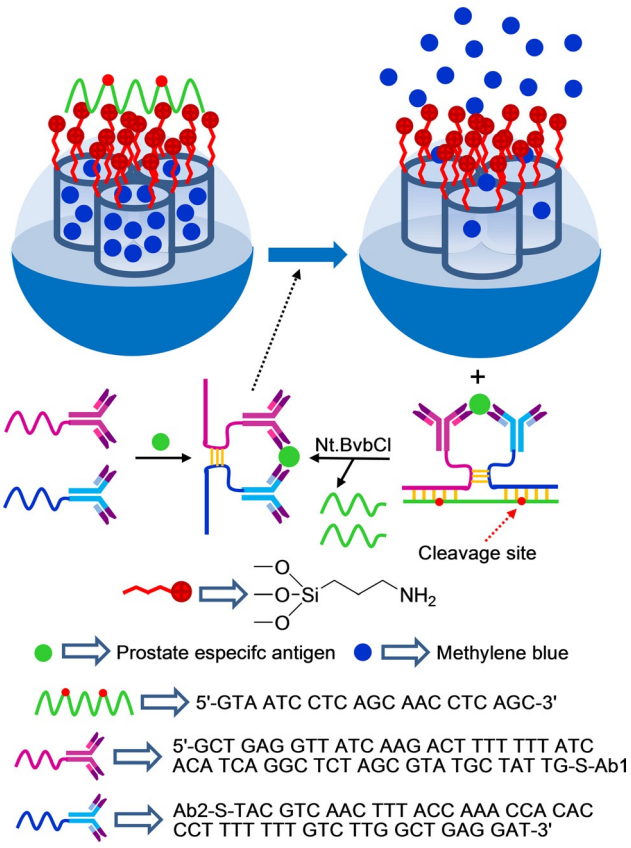


**Figure 32.** Nanometric silica mesoporous support loaded with methylene blue and capped with DNA for the detection of prostate-specific antigen (PSA).

Regarding the use of biomolecules for uncapping protocols, certain examples have been reported where delivery has been selectively observed in the presence of a given enzyme.[57] However, most of these examples have explicitly been prepared for drug delivery, and very few examples for sensing applications have been described. In this context, Ju and co-workers have recently developed a telomerase-responsive gated system for the sensitive in situ tracking of telomerase activity in living cells which, for instance, can be used to distinguish cancer cells from normal cells (see Figure 33).[58] In their

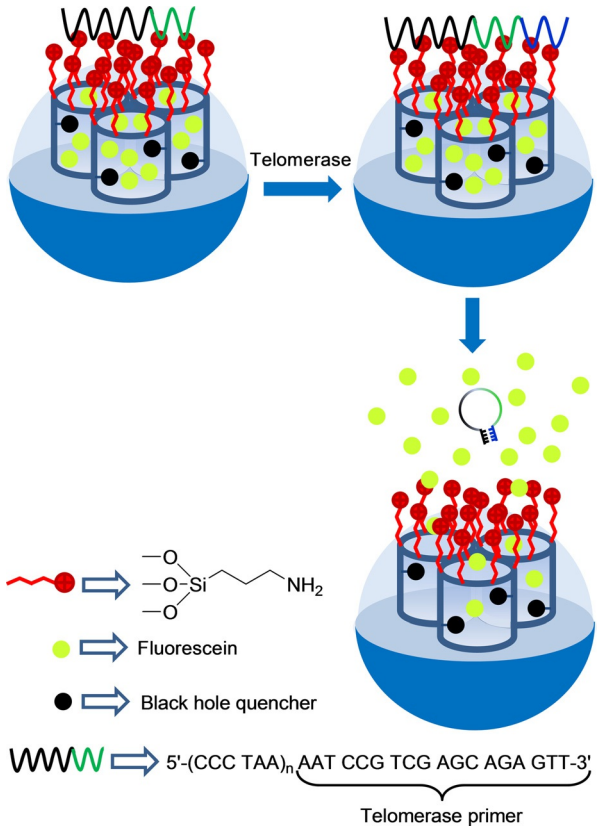


**Figure 33.** Nanometric silica mesoporous support capped with DNA for the detection of telomerase activity.

work, the authors prepared an SMS in the form of nanoparticles, which were functionalized with a fluorescence quencher on inner walls and were loaded with fluorescein. Nanoparticles were functionalized with amino groups on the external surface. The system was capped with DNA sequence 5′-$(CCCTAA)_n$ AATCCG TCGAGC AGAGTT-3′, which contains a telomerase primer, via electrostatic interactions with the amino groups attached to the SMS. In the presence of telomerase and deoxynucleoside triphosphate monomers (dNTPs), the oligonucleotide sequence was extended and formed a rigid hairpin-like DNA structure, which moved away from the SMS surface to allow entrapped fluorescein release. The telomerase-driven response was studied by incubating the enzyme, dNTPs, and capped nanoparticles, and by monitoring fluorescein release by fluorescence and UV/Vis spectroscopy. A gradual increase in fluorescein intensity with a prolonged incubation time was observed, which demonstrated the telomerase-induced release of the cargo. These authors also conducted an extended in vitro study on HeLa cells (cervical cancer cells) using the gated nanoparticles. They concluded that fluorescence due to fluorescein release was activated by the action of intracellular telomerase and suggested that the system could be used for tracking intracellular telomerase activity. These authors also performed different assays with other cell lines, such as BEL-7402 cells (liver cancer cells) and QSG-7701 cells (liver normal cells), which confirmed that the designed strategy can be applied to distinguish cancer cells from normal cells.

Following a similar approach, Lu and co-workers used the same gated design, but loaded the SMS with glucose to monitor telomerase activity with a glucometer.[59] In this case, linear dependence between the glucometer readout and the number of HeLa cells used in the experiment was achieved within the range of 100–5000 cells. The LOD was set at 80 HeLa cells $mL^{-1}$. Finally, Cui and co-workers also prepared a similar material, but used core–shell nanoparticles (in which Au@Ag nanorods were coated with mesoporous silica) and doxorubicin as the payload.[60] These authors also demonstrated the telomerase-induced release of the loaded drug and were able to trace the uptake of the prepared nanoparticles by HeLa cells using surface-enhanced Raman spectroscopy (SERS) measurements.

Willner and co-workers prepared DNA-capped mesoporous silica nanoparticles for the recognition of nucleic acid biomarkers.[61] The external surface of the nanoparticles was functionalized with aminopropyl moieties which were then reacted with a single-stranded DNA sequence (5′-CAA GGG AAG TCT TCA CTG CCC TTG CAC ACT −3′), using *N*-maleimidocaproyl-oxysulfosuccinimide ester (EMCS) as covalent crosslinker. The grafted DNA included a tailored base sequence that generates at room temperature a hairpin structure (blocking the pores) and also included a single-stranded loop able to recognize the nucleic acid biomarker 5′-AGT GTG CAA GGG CAG TGA AGA CTT GAT TGT-3′. The pores were loaded with rhodamine B. Treatment of the capped solid with the biomarker induced the opening of the hairpin forming a duplex structure that also blocked the pores inhibiting dye release. However, in this case, addition of Exo III induced the hydrolysis of the 3′-end of the capping sequence allowing release of the entrapped dye. Using the same approach, other solids functionalized with 5′-AAC GAA GCT GAG GAT GTG TTC GTT-3′ for the biomarker 5′-ATC CTC AGC TTC G-3′ was prepared. Both DNA strands formed a duplex structure that was able to cap the pores and inhibit dye release. In this case the duplex included a programmed sequence for the specific nicking of one base. Upon addition of < the nicking endonuclease Nb.BbvCI, rhodamine B release was observed.

## 6 Conclusions and Outlook

The design of gated mesoporous materials has proved to be a promising starting point for applying the versatility of molecular-based ideas to design nanoscopic gating solids and a way to study factors that can influence the design of molecular

gating functions based on molecular/biomolecular/supramolecular concepts. This review provides an account of examples based on silica mesoporous supports (SMSs) for sensing applications. These new sensing systems are related to the interest in designing gated nanoscopic hybrid materials with the ability to release a previously entrapped cargo when certain external stimuli are applied.

As stated above, most of these functional materials have been used for drug delivery studies. In sensing applications however, the main idea is that the coordination or reaction of a target analyte with the "gate" could modulate the delivery of a reporter from pores to solution, which would result in a suitable easy-to-measure response. One major characteristic in capped sensing SMSs is that cargo delivery should be fast. Whereas delivery should often be sustained over time in most therapeutic applications of gated materials, delivery in sensing systems should be as fast as possible.

In this review, we include examples that have been specifically designed to act as sensing systems by the selective delivery of a reporter. In this context, we have described examples of the sensing of anions, cations, small molecules, and biomolecules. Moreover, we have included some selected examples that, although originally designed for controlled cargo delivery, have displayed some features in terms of selectivity and sensitivity, making them suitable for sensing applications. Capped supports for sensing applications is a developing research area, and a number of new advances in this field are envisioned. In particular, it should be noted that only minor changes are required to transform a controlled-release system, for instance specifically designed for drug delivery, into a sensing material. The crucial issues include achieving selectivity against other analytes, sensitivity, and a fast response time.

In particular, response time is one important issue for the use of these capped materials in real analytical systems, such as test-strip assays or microfluidic devices. Most of the described systems have response times ranging from several minutes (most of them) to hours. A decrease in response time to seconds or very few minutes is thus crucial for real applications. As far as we know, there is only one example of the implementation of capped SMSs in a lateral-flow assay,[44] and further studies need to be carried out regarding response times of these materials in order to advance their use in analytical detection/determination protocols. Moreover, the existence of amplification features, the possibility of using a wide variety of mesoporous supports, and the potential employment of a wide range of reporters able to display a signal (optical, electrochemical, etc.) upon delivery—all these make the possibilities for this approach practically unlimited and highly appealing for the design of new advanced sensing systems for a variety of guests. However, in order to achieve this goal, certain barriers have to be overcome. Further systems to be developed need to be highly selective, have low limits of detection, and display a very short response time.

## Acknowledgements

*The authors gratefully acknowledge financial support from the Spanish Government (Project MAT2012-38429-C04-01) and the Generalitat Valenciana (Project PROMETEOII/2014/047). Ll. P. and M. O. also thank the Universidad Politécnica de Valencia for their predoctoral grants.*

**Keywords:** anions · biomolecules · cations · gated materials · mesoporous silica · sensors

[1] a) E. Katz, I. Willner, *Angew. Chem. Int. Ed.* **2004**, *43*, 6042 – 6108; *Angew. Chem.* **2004**, *116*, 6166 – 6235; b) F. Wang, X. Liu, I. Willner, *Angew. Chem. Int. Ed.* **2015**, *54*, 1098 – 1129; *Angew. Chem.* **2015**, *127*, 1112 – 1144.

[2] A. B. Descalzo, R. Martínez-Máñez, F. Sancnón, K. Hoffmann, K. Rurack, *Angew. Chem. Int. Ed.* **2006**, *45*, 5924 – 5948; *Angew. Chem.* **2006**, *118*, 6068 – 6093.

[3] a) C. H. Lu, B. Willner, I. Willner, *ACS Nano* **2013**, *7*, 8320 – 8332; b) S. Saha, K. C. F. Leung, T. D. Nguyen, J. F. Stoddart, J. I. Zink, *Adv. Funct. Mater.* **2007**, *17*, 685 – 693; c) I. I. Slowing, B. G. Trewyn, S. Giri, V. S. Y. Lin, *Adv. Funct. Mater.* **2007**, *17*, 1225 – 1236; d) S. Angelos, E. Johansson, J. F. Stoddart, J. I. Zink, *Adv. Funct. Mater.* **2007**, *17*, 2261 – 2271; e) B. G. Trewyn, S. Giri, I. I. Slowing, V. S. Y. Lin, *Chem. Commun.* **2007**, 3236 – 3245; f) R. Klajn, J. F. Stoddart, B. A. Grzybowski, *Chem. Soc. Rev.* **2010**, *39*, 2203 – 2237; g) Z. Li, J. C. Barnes, A. Bosoy, J. F. Stoddart, J. I. Zink, *Chem. Soc. Rev.* **2012**, *41*, 2590 – 2605; h) P. Yang, S. Gai, J. Lin, *Chem. Soc. Rev.* **2012**, *41*, 3679 – 3698; i) M. Liong, S. Angelos, E. Choi, K. Patel, J. F. Stoddart, J. I. Zink, *J. Mater. Chem.* **2009**, *19*, 6251 – 6257; j) Q. He, J. Shi, *J. Mater. Chem.* **2011**, *21*, 5845 – 5855; k) Y. W. Yang, *Med. Chem. Commun.* **2011**, *2*, 1033 – 1049; l) J. M. Rosenholm, C. Sahlgren, M. Lindén, *Nanoscale* **2010**, *2*, 1870 – 1883.

[4] a) J. S. Beck, J. C. Vartuli, W. J. Roth, M. E. Leonowicz, C. T. Kresge, K. D. Schmitt, C. T. W. Chu, D. H. Olson, E. W. Sheppard, S. B. McCullen, J. B. Hoggins, J. L. Schlenker, *J. Am. Chem. Soc.* **1992**, *114*, 10834 – 10843; b) A. P. Wight, M. E. Davis, *Chem. Rev.* **2002**, *102*, 3589 – 3614.

[5] a) G. Kickelbick, *Angew. Chem. Int. Ed.* **2004**, *43*, 3102 – 3104; *Angew. Chem.* **2004**, *116*, 3164 – 3166; b) B. G. Trewyn, I. I. Slowing, S. Giri, H. T. Chen, V. S. Y. Lin, *Acc. Chem. Res.* **2007**, *40*, 846 – 853.

[6] E. Aznar, R. Martínez-Máñez, F. Sancenón, *Expert Opin. Drug Delivery* **2009**, *6*, 643 – 655.

[7] C. Coll, A. Bernardos, R. Martínez-Máñz, F. Sancenón, *Acc. Chem. Res.* **2013**, *46*, 339 – 349.

[8] For molecular sensors see for example: a) L. E. Santos-Figueroa, M. E. Moragues, E. Climent, A. Agostini, R. Martínez-Máñez, F. Sancenón, *Chem. Soc. Rev.* **2013**, *42*, 3489 – 3613; b) M. E. Moragues, R. Martínez-Máñez, F. Sancenón, *Chem. Soc. Rev.* **2011**, *40*, 2593 – 2643; c) Y. Salinas, R. Martínez-Máñez, M. D. Marcos, F. Sancenón, A. M. Costero, M. Parra, S. Gil, *Chem. Soc. Rev.* **2012**, *41*, 1261 – 1296; d) S. K. Kim, D. H. Lee, J. I. Hong, J. Yoon, *Acc. Chem. Res.* **2009**, *42*, 23 – 31; e) X. Chen, Y. Zhou, X. Peng, J. Yoon, *Chem. Soc. Rev.* **2010**, *39*, 2120 – 2135; f) A. P. de Silva, H. Q. N. Gunaratne, T. Guunnlaugsson, A. J. M. Huxley, C. P. McCoy, J. T. Rademacher, T. E. Rice, *Chem. Rev.* **1997**, *97*, 1515 – 1566; g) R. Martínez-Máñez, F. Sancenón, *Chem. Rev.* **2003**, *103*, 4419 – 4476.

[9] M. Hecht, E. Climent, M. Biyical, F. Sancenón, R. Martínez-Máñez, K. Rurack, *Coord. Chem. Rev.* **2013**, *257*, 2589 – 2606.

[10] See for example: a) G. Wang, L. Wang, Y. Han, S. Zhou, X. Guan, *Acc. Chem. Res.* **2013**, *46*, 2867 – 2877; b) A. Liu, Q. Zhao, X. Guan, *Anal. Chim. Acta* **2010**, *675*, 106 – 115; c) S. Matile, H. Tanaka, S. Litvinchuk, *Top. Curr. Chem.* **2007**, *277*, 219 – 250; d) A. Destexhe, D. Contreras, *Science* **2006**, *314*, 85 – 90; e) H. Bayley, O. Braha, L. Q. Gu, *Adv. Mater.* **2000**, *12*, 139 – 142.

[11] See for example: a) R. Martínez-Máñez, F. Sancenón, M. Biyical, M. Hecht, K. Rurack, *J. Mater. Chem.* **2011**, *21*, 12588 – 12604; b) R. Martínez-Máñez, F. Sancenón, M. Biyical, M. Hecht, K. Rurack, *Anal. Bioanal. Chem.* **2011**, *399*, 55 – 74.

[12] See for example: a) S. Amemiya, Y. Wang, M. V. Mirkin in *Electrochemistry, Vol. 12*, (Eds.: J. D. Wadhawan, R. G. Compton), RSC Publishing, Cam-

 

bridge (UK), **2014**, Chapter 1., p. 1–43; b) D. Tonelli, E. Scavetta, M. Giorgetti, *Anal. Bioanal. Chem.* **2013**, *405*, 603–614; c) M. Scampicchio, A. Bulbanello, A. Arecchi, M. S. Cosio, S. Benedetti, S. Mannino, *Electroanalysis* **2012**, *24*, 719–725; d) B. M. Venkatesan, R. Bashir, *Nat. Nanotechnol.* **2011**, *6*, 615–624.

[13] R. Casasús, E. Aznar, M. D. Marcos, R. Martínez-Máñez, F. Sancenón, J. Soto, P. Amorós, *Angew. Chem. Int. Ed.* **2006**, *45*, 6661–6664; *Angew. Chem.* **2006**, *118*, 6813–6816.

[14] R. Casasús, E. Climent, M. D. Marcos, R. Martínez-Máñez, F. Sancenón, J. Soto, P. Amorós, J. Cano, E. Ruiz, *J. Am. Chem. Soc.* **2008**, *130*, 1903–1917.

[15] C. Coll, R. Casasús, E. Aznar, M. D. Marcos, R. Martínez-Máñez, F. Sancenón, J. Soto, P. Amorós, *Chem. Commun.* **2007**, 1957–1959.

[16] C. Coll, E. Aznar, R. Martínez-Máñez, M. D. Marcos, F. Sancenón, J. Soto, P. Amorós, J. Cano, E. Ruiz, *Chem. Eur. J.* **2010**, *16*, 10048–10061.

[17] E. Aznar, C. Coll, M. D. Marcos, R. Martínez-Máñez, F. Sancenón, J. Soto, P. Amorós, J. Cano, E. Ruiz, *Chem. Eur. J.* **2009**, *15*, 6877–6888.

[18] V. C. Özalp, T. Schäfer, *Chem. Eur. J.* **2011**, *17*, 9893–9896.

[19] V. C. Özalp, A. Pinto, E. Nikulina, A. Chuvilin, T. Schäfer, *Part. Part. Syst. Charact.* **2014**, *31*, 161–167.

[20] X. He, Y. Zhao, D. He, K. Wang, F. Xu, J. Tang, *Langmuir* **2012**, *28*, 12909–12915.

[21] C. L. Zhu, C. H. Lu, X. Y. Song, H. H. Yang, X. R. Wang, *J. Am. Chem. Soc.* **2011**, *133*, 1278–1281.

[22] L. Hou, C. Zhu, X. Wu, G. Chen, D. Tang, *Chem. Commun.* **2014**, *50*, 1441–1443.

[23] E. Climent, M. D. Marcos, R. Martinez-Máñez, F. Sancenón, J. Soto, K. Rurack, P. Amorós, *Angew. Chem. Int. Ed.* **2009**, *48*, 8519–8522; *Angew. Chem.* **2009**, *121*, 8671–8674.

[24] Y. F. Zhang, Q. Yuan, T. Chen, X. B. Zhang, Y. Chen, W. H. Tan, *Anal. Chem.* **2012**, *84*, 1956–1962.

[25] Y. Wen, L. Xu, C. Li, H. Du, L. Chen, B. Su, Z. Zhang, X. Zhang, Y. Song, *Chem. Commun.* **2012**, *48*, 8410–8412.

[26] Y. L. Choi, J. Jaworski, M. L. Seo, S. J. Lee, J. H. Jung, *J. Mater. Chem.* **2011**, *21*, 7882–7885.

[27] Z. Zhang, F. Wang, D. Balogh, I. Willner, *J. Mater. Chem. B* **2014**, *2*, 4449–4455.

[28] Z. Zhang, D. Balogh, F. Wang, I. Willner, *J. Am. Chem. Soc.* **2013**, *135*, 1934–1940.

[29] L. Fu, J. Zhuang, W. Lai, X. Que, M. Lu, D. Tang, *J. Mater. Chem. B* **2013**, *1*, 6123–6128.

[30] M. Chen, C. Huang, C. He, W. Zhu, Y. Xu, Y. Lu, *Chem. Commun.* **2012**, *48*, 9522–9524.

[31] E. Aznar, R. Villalonga, C. Gimenez, F. Sancenón, M. D. Marcos, R. Martínez-Máñez, P. Diez, J. M. Pingarron, P. Amorós, *Chem. Commun.* **2013**, *49*, 6391–6393.

[32] R. Villalonga, P. Díez, A. Sánchez, E. Aznar, R. Martínz-Máñez, J. M. Pingarrón, *Chem. Eur. J.* **2013**, *19*, 7889–7894.

[33] P. Díez, A. Sánchez, M. Gamella, P. Martínez-Ruíz, E. Aznar, C. de La Torre, J. R. Murguía, R. Martínez-Máñez, R. Villalonga, M. J. Pingarrón, *J. Am. Chem. Soc.* **2014**, *136*, 9116–9123.

[34] J. Lee, J. Lee, S. Kim, C. J. Kim, S. Lee, B. Min, Y. Shin, C. Kim, *Bull. Korean Chem. Soc.* **2011**, *32*, 1357–1360.

[35] Y. N. Zhao, B. G. Trewyn, I. I. Slowing, V. S. Y. Lin, *J. Am. Chem. Soc.* **2009**, *131*, 8398–8400.

[36] W. Zhao, H. Zhang, Q. He, Y. Li, J. Gu, L. Li, H. Li, J. Shi, *Chem. Commun.* **2011**, *47*, 9459–9461.

[37] S. El Sayed, C. Giménez, E. Aznar, R. Martínez-Máñez, F. Sancenón, M. Licchelli, *Org. Biomol. Chem.* **2015**, *13*, 1017–1021.

[38] Y. Salinas, A. Agostini, E. Pérez-Esteve, R. Martínez-Máñez, F. Sancenón, M. D. Marcos, J. Soto, A. M. Costero, S. Gil, M. Parra, P. Amorós, *J. Mater. Chem. A* **2013**, *1*, 3561–3564.

[39] Y. Salinas, R. Martínez-Máñez, J. O. Jeppesen, L. H. Petersen, F. Sancenón, M. D. Marcos, J. Soto, C. Guillem, P. Amorós, *ACS Appl. Mater. Interfaces* **2013**, *5*, 1538–1543.

[40] Y. Salinas, M. V. Solano, R. E. Sorensen, K. R. Larsen, J. Lycoops, J. O. Jeppesen, R. Martínez-Máñez, F. Sancenón, M. D. Marcos, P. Amorós, C. Guillem, *Chem. Eur. J.* **2014**, *20*, 855–866.

[41] I. Candel, A. Bernardos, E. Climent, M. D. Marcos, R. Martínez-Máñez, F. Sancenón, J. Soto, A. M. Costero, S. Gil, M. Parra, *Chem. Commun.* **2011**, *47*, 8313–8315.

[42] E. Climent, A. Bernardos, R. Martínez-Máñez, A. Maquieira, M. D. Marcos, N. Pastor-Navarro, R. Puchades, F. Sancenón, J. Soto, P. Amorós, *J. Am. Chem. Soc.* **2009**, *131*, 14075–14080.

[43] E. Climent, R. Martínez-Máñez, A. Maquieira, F. Sancenón, M. D. Marcos, E. M. Brun, J. Soto, P. Amorós, *ChemistryOpen* **2012**, *1*, 251–259.

[44] E. Climent, D. Groninger, M. Hecht, M. A. Walter, R. Martínez-Máñez, M. G. Weller, F. Sancenón, P. Amorós, K. Rurack, *Chem. Eur. J.* **2013**, *19*, 4117–4122.

[45] B. Zhang, B. Liu, J. Liao, G. Chen, D. Tang, *Anal. Chem.* **2013**, *85*, 9245–9252.

[46] Z. Gao, D. Tang, M. Xu, G. Chen, H. Yang, *Chem. Commun.* **2014**, *50*, 6256–6258.

[47] D. Tang, Y. Lin, Q. Zhou, Y. Lin, P. Li, R. Niessner, D. Knopp, *Anal. Chem.* **2014**, *86*, 11451–11458.

[48] D. Tang, B. Q. Liu, R. Niessner, P. W. Li, D. Knopp, *Anal. Chem.* **2013**, *85*, 10589–10596.

[49] L. Chen, Y. Wen, B. Su, J. Di, Y. Song, L. Jiang, *J. Mater. Chem.* **2011**, *21*, 13811–13816.

[50] E. Climent, R. Martínez-Máñez, F. Sancenón, M. D. Marcos, J. Soto, A. Maquieira, P. Amorós, *Angew. Chem. Int. Ed.* **2010**, *49*, 7281–7283; *Angew. Chem.* **2010**, *122*, 7439–7441.

[51] E. Climent, L. Mondragón, R. Martínez-Máñez, F. Sancenón, M. D. Marcos, J. R. Murguía, P. Amorós, K. Rurack, E. Pérez-Payá, *Angew. Chem. Int. Ed.* **2013**, *52*, 8938–8942; *Angew. Chem.* **2013**, *125*, 9106–9110.

[52] L. Pascual, I. Baroja, E. Aznar, F. Sancenón, M. D. Marcos, J. R. Murguía, P. Amorós, K. Rurack, R. Martínez-Máñez, *Chem. Commun.* **2015**, *51*, 1414–1416.

[53] Z. Wang, X. Yang, J. Feng, Y. Tang, Y. Jiang, N. He, *Analyst* **2014**, *139*, 6088–6091.

[54] M. Oroval, E. Climent, C. Coll, R. Eritja, A. Aviñó, M. D. Marcos, F. Sancenón, R. Martínez-Máñez, P. Amorós, *Chem. Commun.* **2013**, *49*, 5480–5482.

[55] X. Yang, A. Wang, J. Liu, *Talanta* **2013**, *114*, 5–10.

[56] K. Ren, J. Wu, Y. Zhang, F. Yan, H. Ju, *Anal. Chem.* **2014**, *86*, 7494–7499.

[57] See for example: a) K. Patel, S. Angelos, W. R. Dichtel, A. Coskun, Y. W. Yang, J. I. Zink, J. F. Stoddart, *J. Am. Chem. Soc.* **2008**, *130*, 2382–2383; b) A. Schlossbauer, J. Kecht, T. Bein, *Angew. Chem. Int. Ed.* **2009**, *48*, 3092–3095; *Angew. Chem.* **2009**, *121*, 3138–3141; c) C. Coll, L. Mondragón, R. Martínez-Máñez, F. Sancenón, M. D. Marcos, J. Soto, P. Amorós, E. Pérez-Payá, *Angew. Chem. Int. Ed.* **2011**, *50*, 2138–2140; *Angew. Chem.* **2011**, *123*, 2186–2188; d) A. Agostini, L. Mondragón, A. Bernardos, R. Martínez-Máñez, M. D. Marcos, F. Sancenón, J. Soto, A. Costero, C. Manguan-García, R. Perona, M. Moreno-Torres, R. Aparicio-Sanchis, J. R. Murguía, *Angew. Chem. Int. Ed.* **2012**, *51*, 10556–10560; *Angew. Chem.* **2012**, *124*, 10708–10712; e) P. D. Thornton, A. Heise, *J. Am. Chem. Soc.* **2010**, *132*, 2024–2038; f) Z. Chen, Z. Li, Y. Lin, M. Yin, J. Ren, X. Qu, *Chem. Eur. J.* **2013**, *19*, 1778–1783.

[58] R. Qian, I. Ding, H. Ju, *J. Am. Chem. Soc.* **2013**, *135*, 13282–13285.

[59] Y. Wang, M. Lu, J. Zhu, S. Tian, *J. Mater. Chem. B* **2014**, *2*, 5847–5853.

[60] S. Zong, Z. Wang, H. Chen, D. Zhu, P. Chen, Y. Cui, *IEEE Trans. Nanobiosci.* **2014**, *13*, 55–60.

[61] Z. Zhang, D. Balogh, F. Wang, S. Y. Sung, R. Nechushtai, I. Willner, *ACS Nano* **2013**, *7*, 8455–8468.

Received: February 23, 2015
Published online on June 12, 2015

 